PHENOTYPE OF UTERINE FIBROIDS AND CLINICAL SYMPTOMS

The basic science, ***Pasquapina Ciarmela (Italy)***

UNIVERSITÀ POLITECNICA DELLE MARCHE

Leiomyoma → leio (smooth) + myo (muscle) + oma (tumor)

- Well circumscribed benign masses
- Single or multiple masses
- Whirled, shiny, white, bulging, rubbery cut surface

- Composed of irregular bundles of cells in an extensive tissue matrix

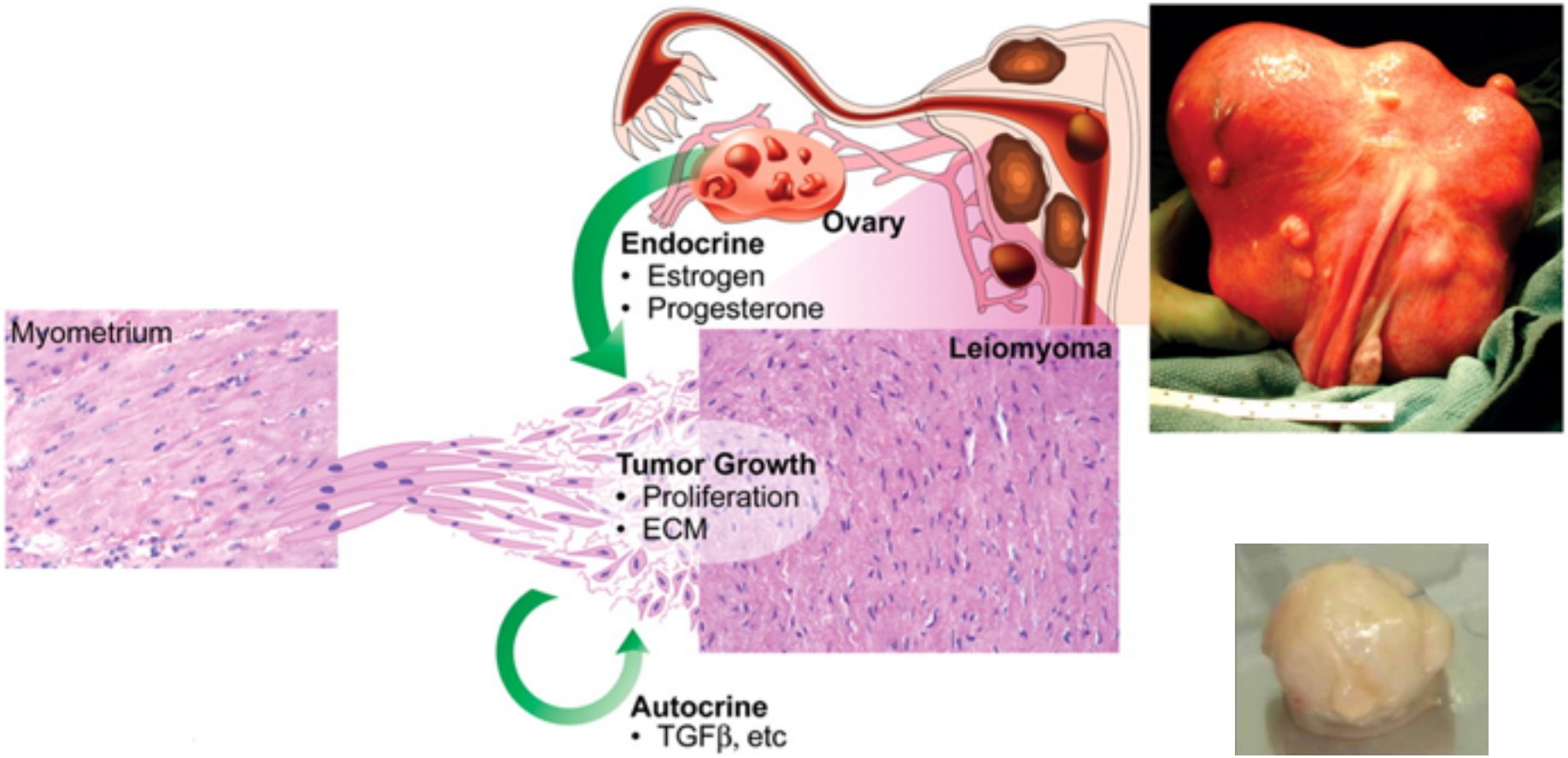

Etiology of uterine fibroids. Tumor growth occurs by an increase in tumor cell number and ECM production and is promoted by both endocrine and autocrine growth factors.

Modified by: Walker CL, Stewart EA. Uterine fibroids: the elephant in the room. Science. 2005; 308:1589-92. Review.

ECM

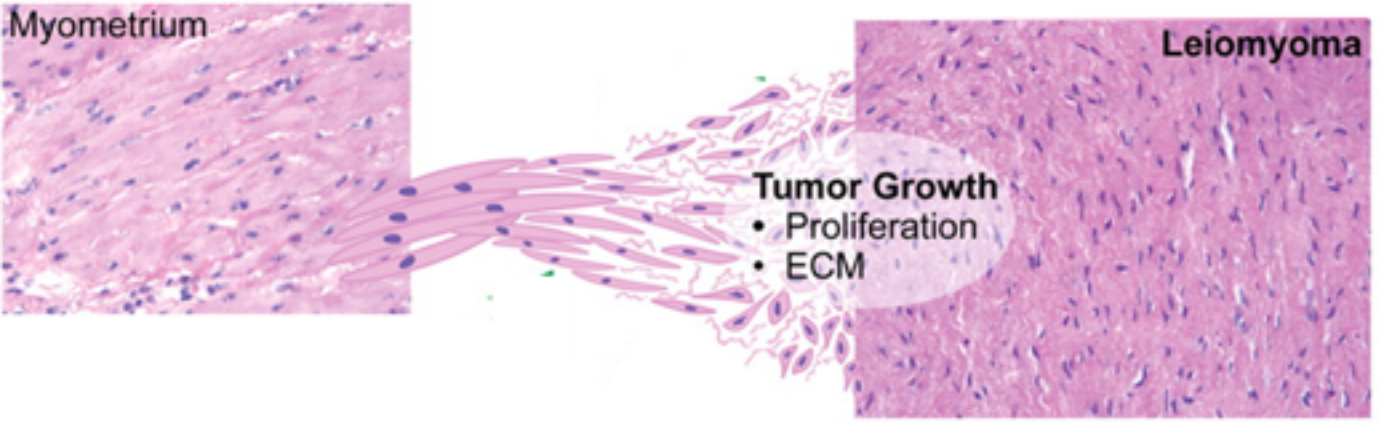

The ECM synthesis is an important event in leiomyoma growth.

Recent studies suggest that alterations in ECM can modify mechanical stress on cells, which leads to activation of internal mechanical signaling contributing to leiomyoma.

Primarily collagens, fibronectin, and proteoglycans have been found in leiomyoma with altered expression compared with normal myometrium.

Leiomyoma

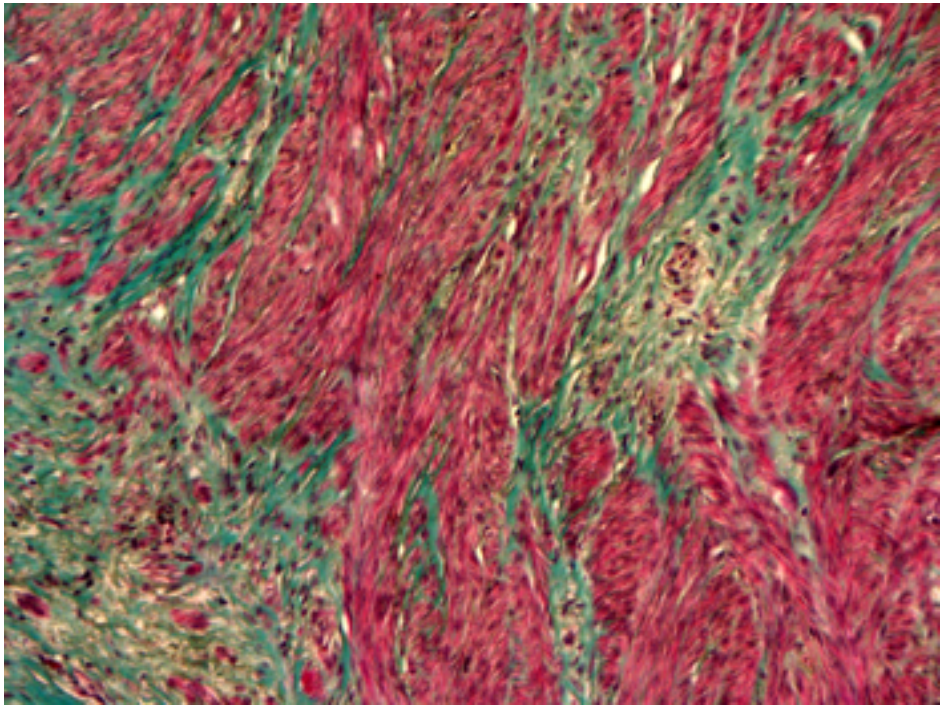

Myometrium

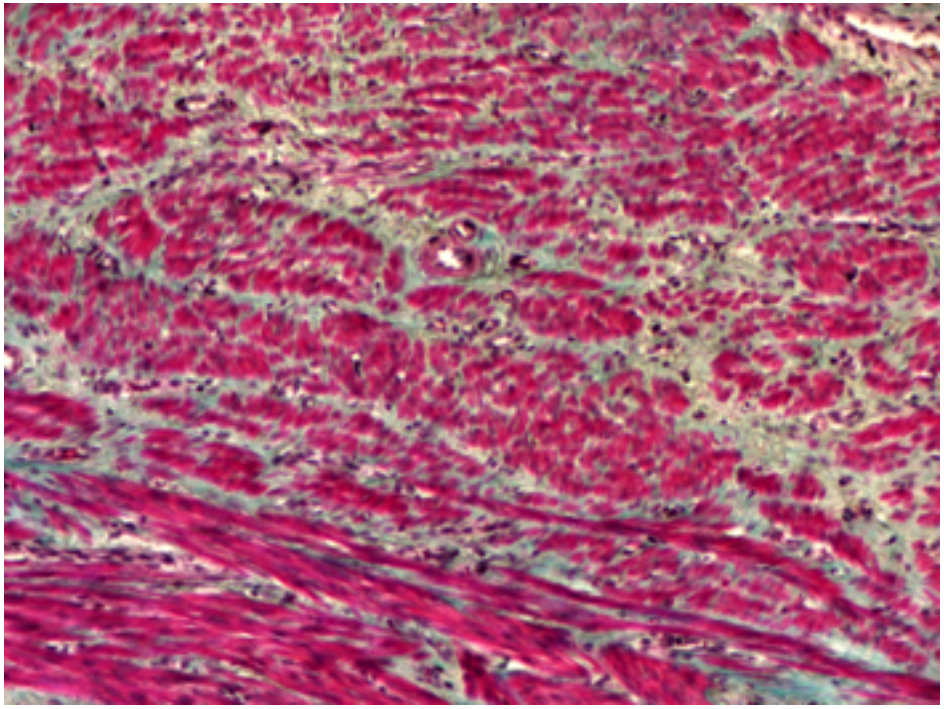

Collagen consistency and deposition in leiomyoma and corresponding myometrium. Masson's trichrome stain highlights green=collagen and red=smooth muscle.

A Phase-Contrast based High-Resolution X-Ray Tomography Study

Synchrotron is an extremely powerful source of X-ray produced by highly energetic electrons moving in a large circular installation.

A synchrotron facility serves to accelerate electrons to extremely high energy and then make them change direction periodically under the action of a magnetic field.

ELETTRA
Italian Synchrotron Radiation Facility

Basovizza (TS), Italy

Dr.ssa Alessandra Giuliani
Applied Physics

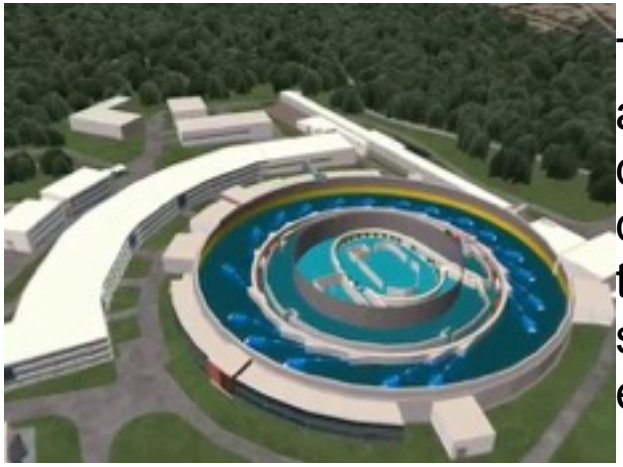

The resulting X-rays are emitted and directed toward the different beamlines that surround the storage ring in the experimental hall.

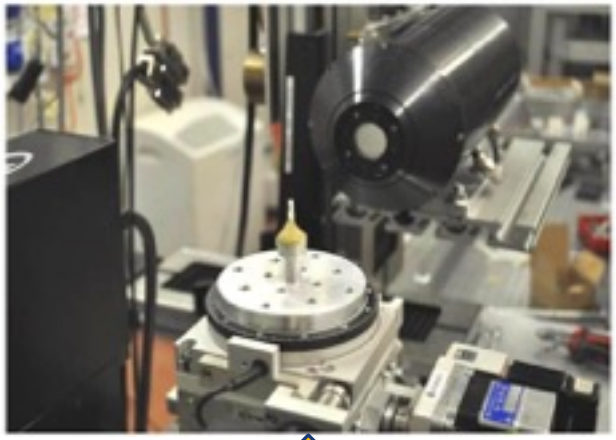

The SYRMEP SYnchrotron Radiation for MEdical Physics beamline

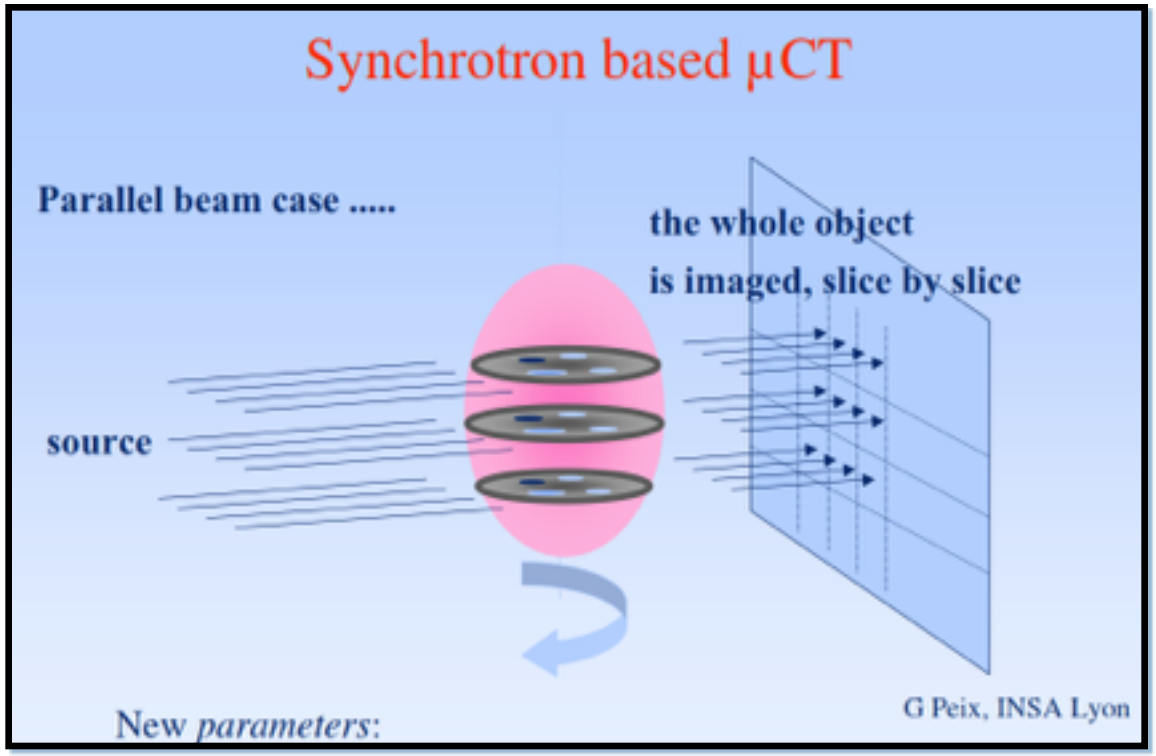

Micro-CT is similar to conventional CT usually used in medical diagnosis but, unlike CT systems, which typically reach the spatial resolution of about 0.5 mm, micro-CT is capable of achieving a spatial resolution up to 0.2-0.3 micron, i.e., about three orders of magnitude lower.

Micro-CT allows high spatial resolution images to be generated with high signal-to-noise ratio, permitting also to perform density measurements after several standard calibration measurements.

Experimental setups

Parallel beam:

Absorption Tomography

Phase Contrast Tomography

Resolution limited by *detector*

500 nm best

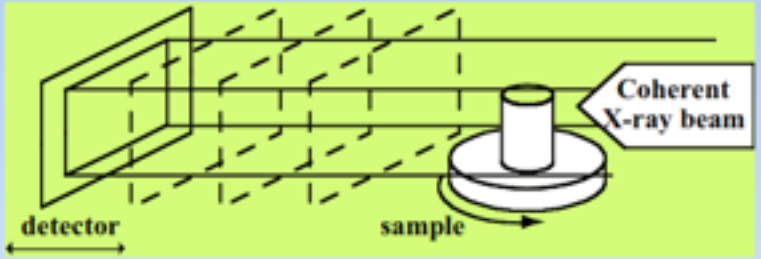

Phase-Contrast vs Absorption Imaging

Advantages

The spatial coherence of the SYRMEP source is used to overcome the poor absorption contrast of many biological samples (i.e. non-mineralized tissues), by the use of phase-contrast techniques.

Leiomyoma

Myometrium

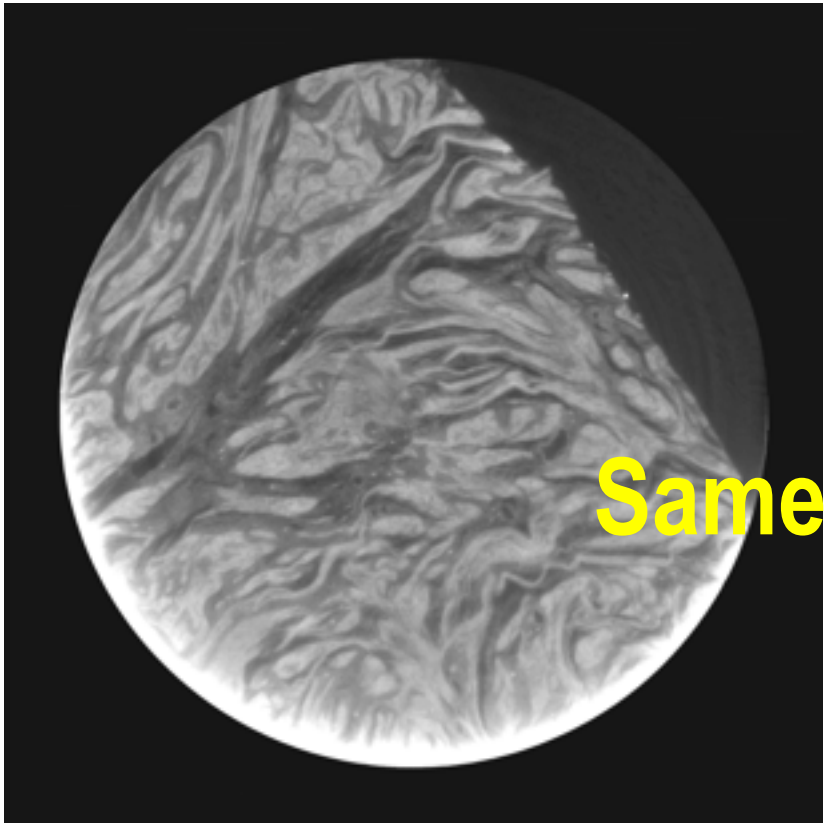

Same patient!

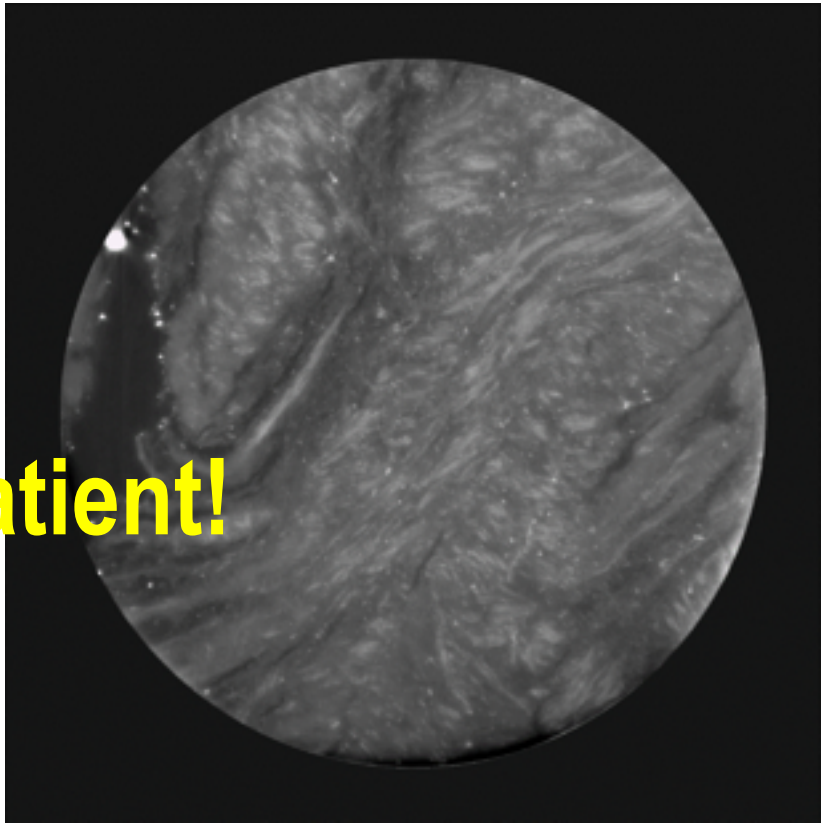

500 µm

Leiomyoma*

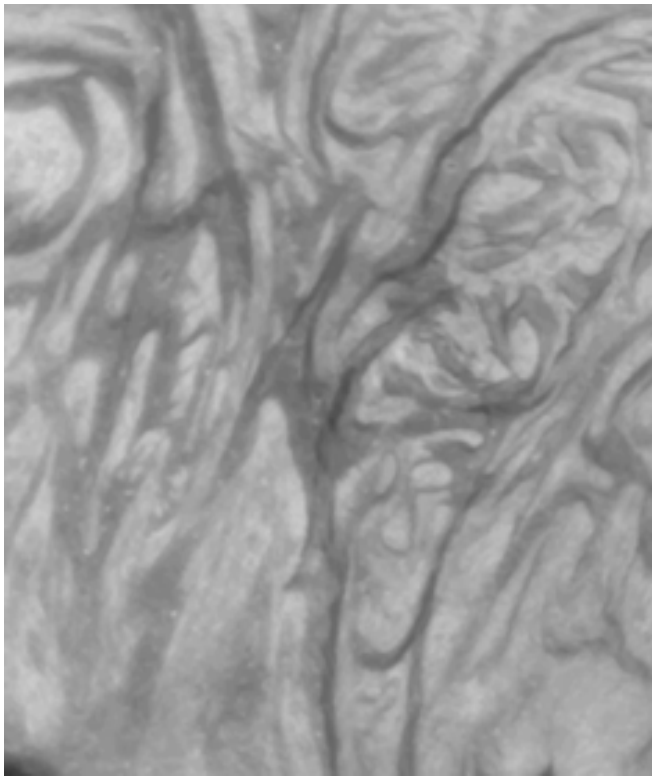

Myometrium*

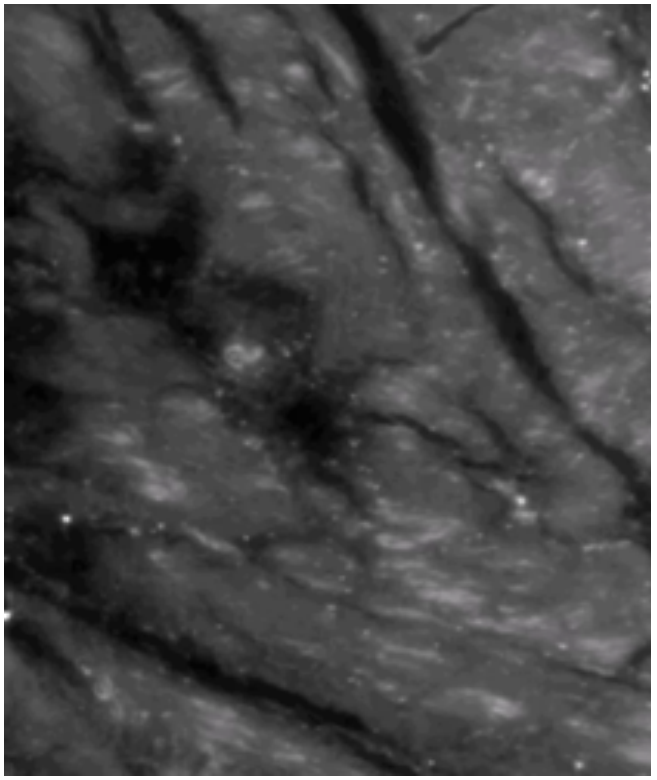

* Around 700 2D-slices, 800x1000 μm^2 each

Leiomyoma

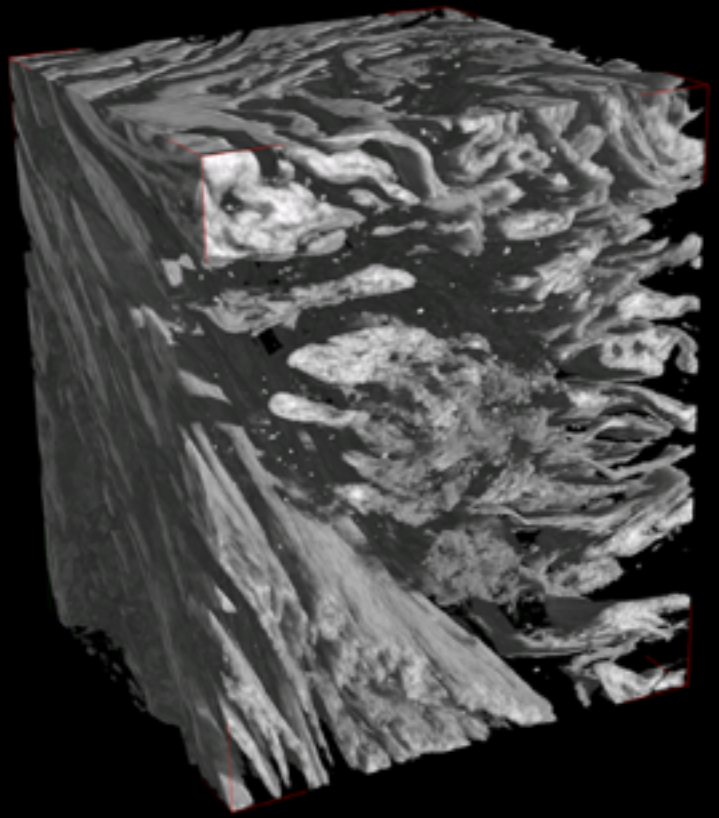

Myometrium

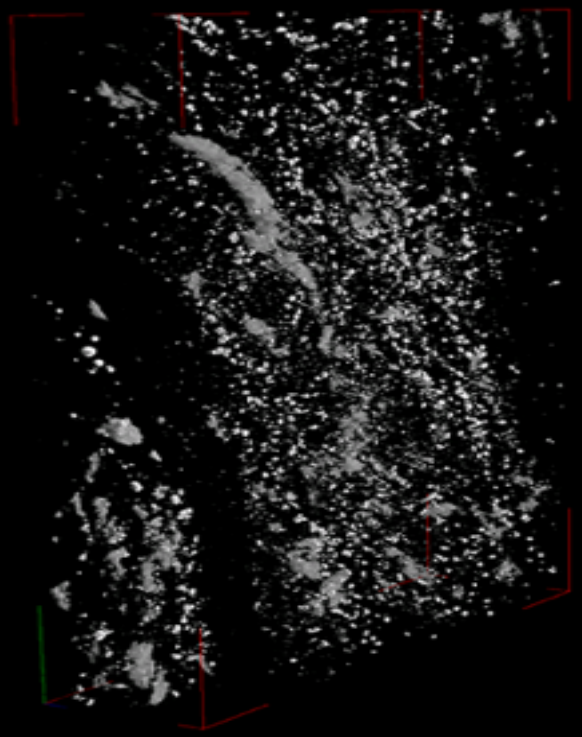

Mass density study extrapolating relative Mass Density Distribution (MDD^r)

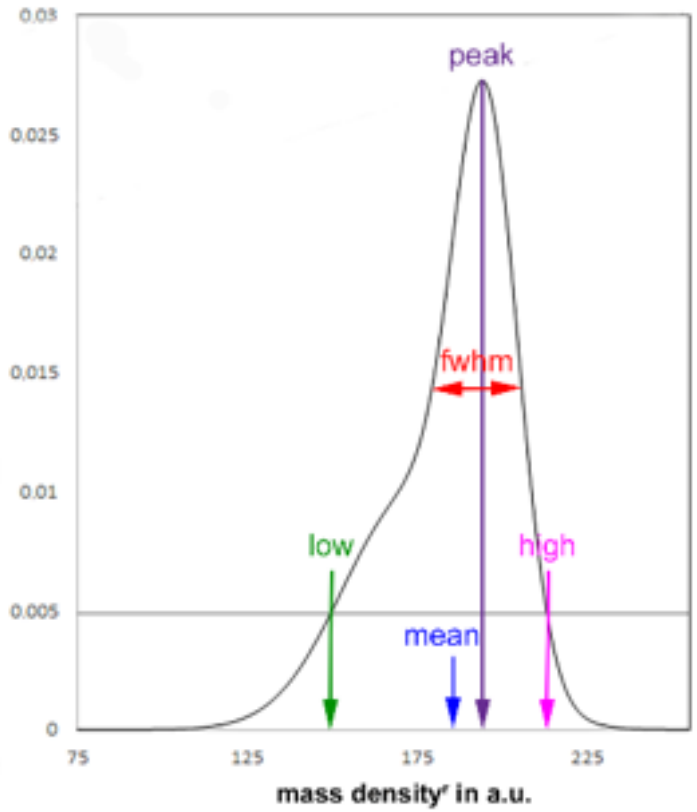

	LM	MM
MDD$^r_{mean}$ in a.u.	141	105
MDD$^r_{peak}$ in a.u.	160	105
MDD$^r_{fwhm}$ in a.u	72	42
MDD$^r_{low}$ in a.u.	69	63
MDD$^r_{high}$ in a.u.	213	147

Following the Roschger approach, previously used for bone tissue, five parameters were extracted from the MDD^r: the mean relative mass density (MDD$^r_{mean}$), the most frequent relative mass density value (MDD$^r_{peak}$), the 0.5th (MDD$^r_{low}$) and the 99.5th (MDD$^r_{high}$) percentiles, and the full width at half maxima of the distribution (MDD$^r_{fwhm}$). This post-processing calculation of the MDD^r parameters was done using the PeakFit software (Systat Software, San Jose, CA).

Morfometric analysis of collagen distribution by segmentation of the histograms refered to the study of mass density.

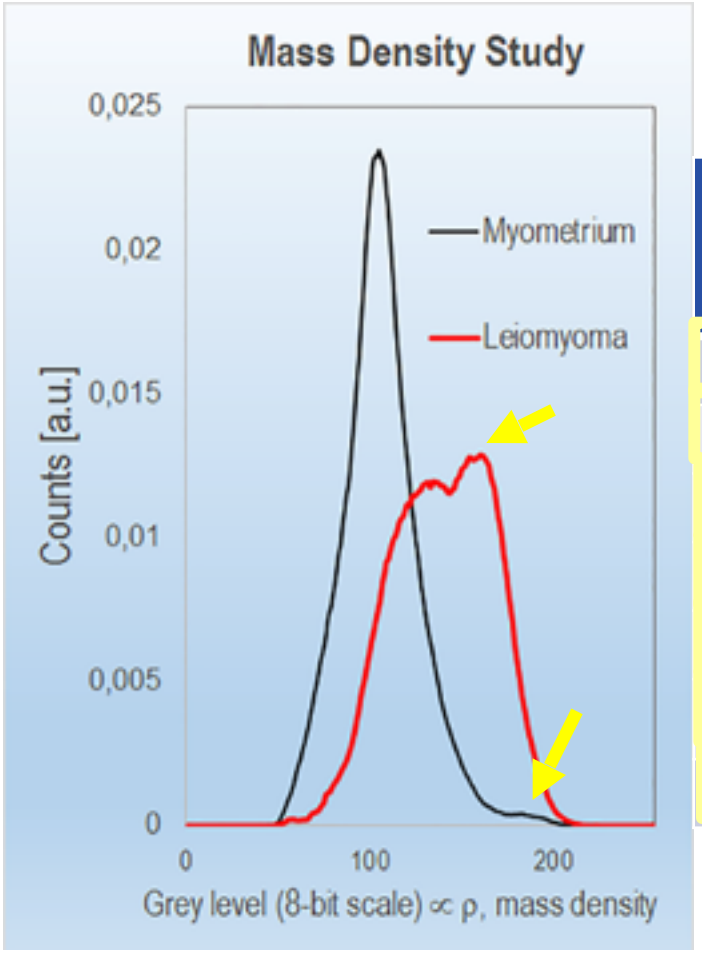

Collagen Quantification

	Leiomyoma	Myometrium
CollFb_V/TV (%)	41.6 (0.2)	2.0 (1.3)
CollFb_S/CollFb_V (mm-1)	120 (11)	418 (29)
CollFb_Th (um)	17 (1)	6 (4)
CollFb_Nr (mm-1)	25 (3)	3 (0)
CollFb_Sp (um)	22.5 (0.7)	301.5 (14.8)
CollFb_ConnD (mm-3)	5.51E+3 (3.63E+3)	0.11E+3 (0.14E+3)
CollFb_DA	0.717 (0.024)	0.397 (0.106)

* Mean (Std.Dev.)

Finally, as Collagen Fibers could vary their orientation depending on the pathology, we also extracted information about the anisotropy of the collagen structure, i.e. the presence of preferential orientation(s). The anisotropy degree index (**CollFb_DA**) measures the similarity of a fabric to a uniform distribution and varies between 0 (all observation confined to a single plane or axis) and 1 (perfect isotropy).The CollFb_DA analysis was performed using the BoneJ Plugin of the ImageJ software, version 3.

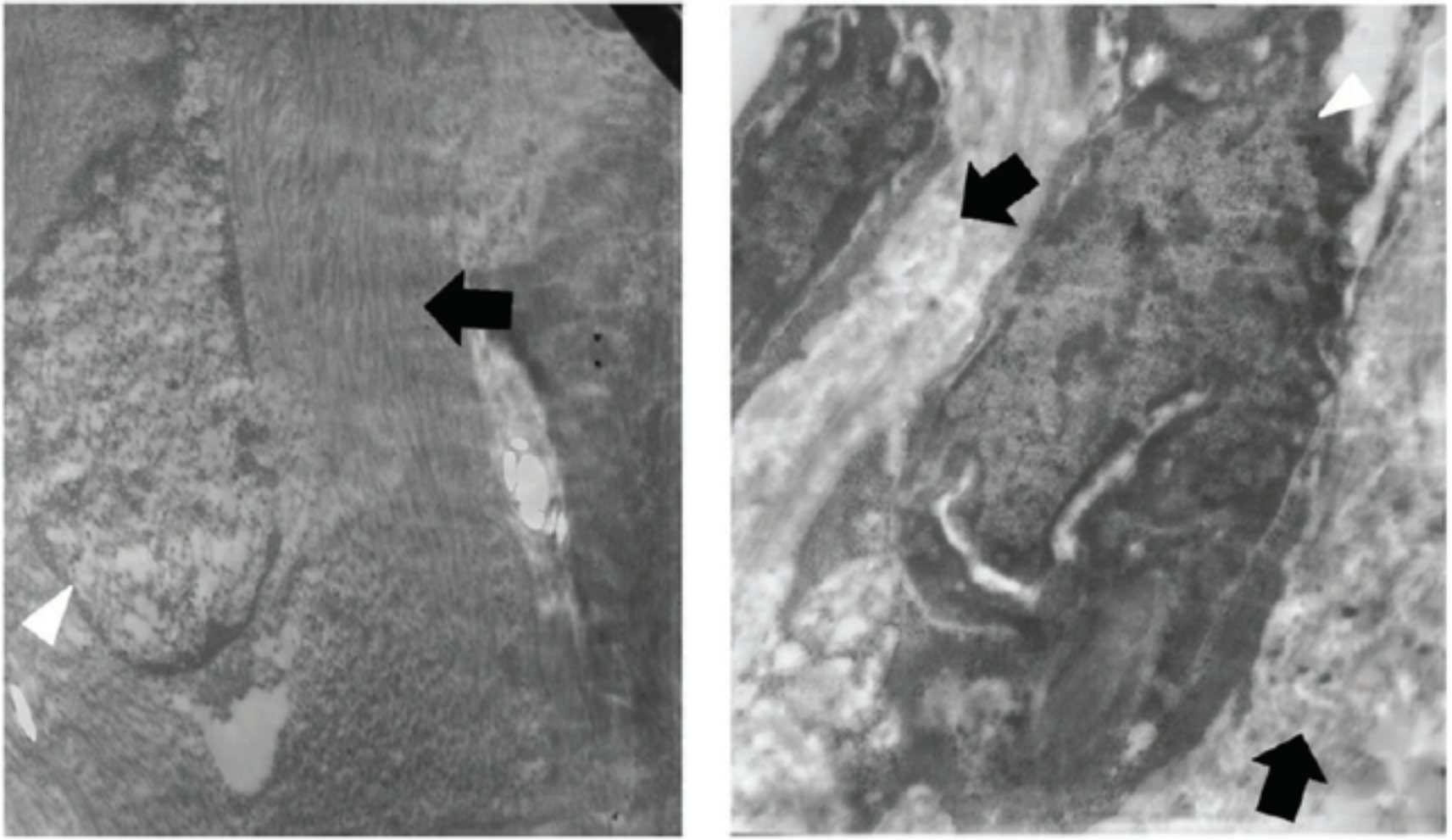

(a) (b)

Collagen fibrils in myometrium and fibroids. Comparison of collagen fibril organization in the extracellular matrix of myometrium or uterine fibroid using electron microscopy. (a) Myometrium. Collagen fibrils are tightly packed and well-aligned, as shown by the black arrow. The nucleus is denoted by the white arrowhead. Magnification = 11,500x. (b) Fibroid. The collagen fibrils are randomly aligned and widely spaced, as shown by black arrows.The nucleus is notched and denoted by thewhite arrowhead.Magnification = 15,500x. Representative sections on samples harvested from a single uterus.

The extracellular matrix contributes to mechanotransduction in uterine fibroids. Leppert PC, Jayes FL, Segars JH. Obstet Gynecol Int. 2014;2014:783289

A new hypothesis about the origin of uterine fibroids based on gene expression profiling with microarrays. Leppert PC, Catherino WH, Segars JH. Am J Obstet Gynecol. 2006;195:415-20

Leiomyomas may develop from a disorder in wound healing process, similar to keloid formation

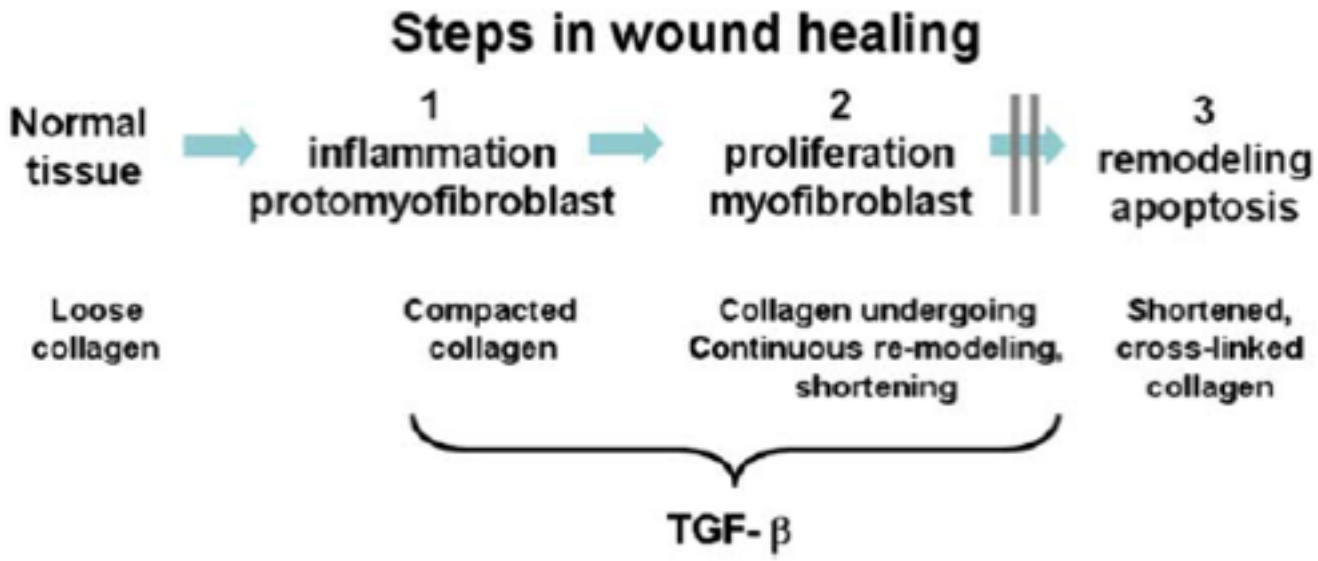

Model of abnormal wound healing in fibroids. Tissue repair is a tightly regulated process with progressive differentiation of cells secreting the ECM, and production of an ECM that is caple of bearing stress. Collagen remodeling is a key feature of repair and TGF-beta plays a critical role in production of the fibrosis associated with healing. Myofibroblasts are highly differentiated cells that undergo apoptosis at completion of the repair, but arrest in differentiation before the final stages of differentiation may result in continued secretion of collagen and excessive fibrosis.

Catherino WH, Leppert PC, Stenmark MH, Payson M, Potlog-Nahari C, Nieman LK, Segars JH. Reduced dermatopontin expression is a molecular link between uterine leiomyomas and keloids. Genes Chromosomes Cancer 2004;40:204-217.

Leppert PC, Baginski T, Prupas C, Catherino WH, Pletcher S, Segars JH. Comparative ultrastructure of collagen fibrils in uterine leiomyomas and normal myometrium. Fertil Steril 2004;82 Suppl 3:1182-7.

A new hypothesis about the origin of uterine fibroids based on gene expression profiling with microarrays. Leppert PC, Catherino WH, Segars JH. Am J Obstet Gynecol. 2006;195:415-20.

Disordered collagen in uterine leiomyomas and keloids

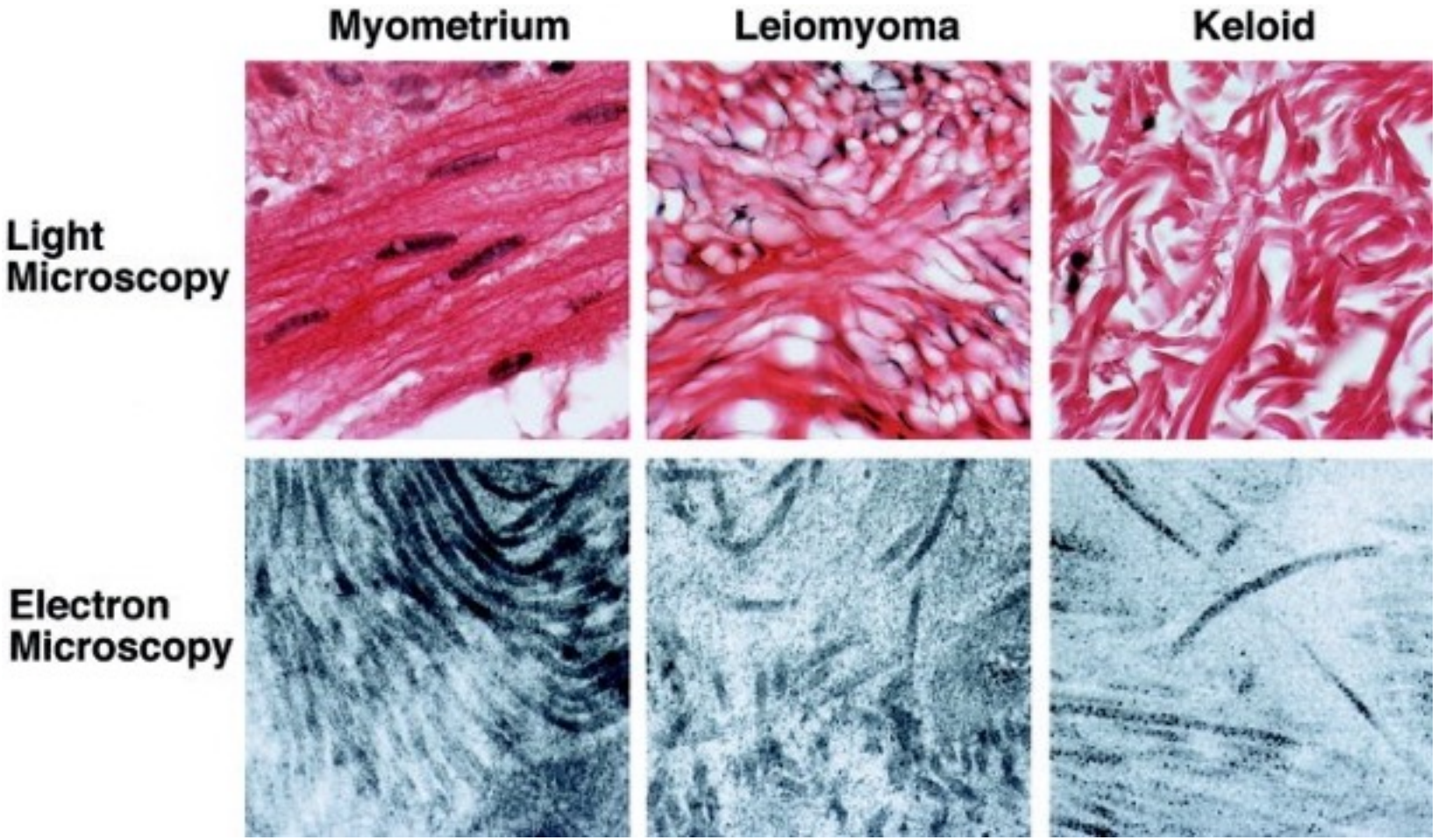

Representative light microscopy with hematoxylin/eosin staining (top row) and electron microscopy (bottom row) comparing myometrium, leiomyoma, and keloid. Myometrium and leiomyoma are from patient 11; keloid is from an African–American patient who underwent surgical extirpation of keloid tissue. Disordered collagen was present in leiomyoma and keloid matrix, whereas ordered collagen bundles were present in the extracellular matrix of the myometrium (light microscopy—63× magnification, electron microscopy—41,000× magnification).

Reduced dermatopontin expression is a molecular link between uterine leiomyomas and keloids. Catherino WH, Leppert PC, Stenmark MH, Payson M, Potlog-Nahari C, Nieman LK, Segars JH. Genes Chromosomes Cancer. 2004;40:204-17

Hypothetical presentation of fibrosis in uterine leiomyoma

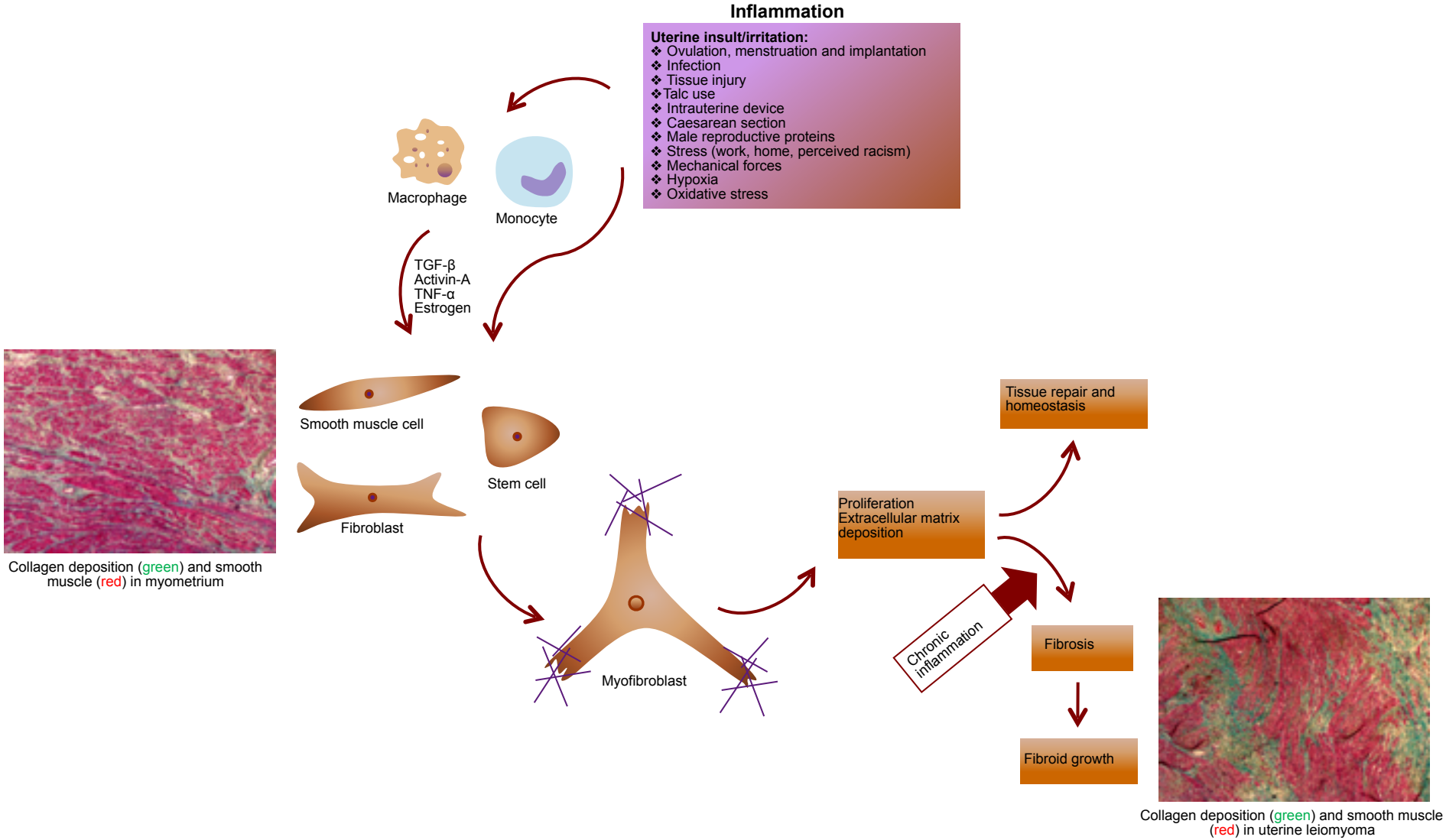

Islam MS, Ciavattini A, Petraglia F, Castellucci M and Ciarmela P. Extracellular matrix in uterine leiomyoma pathogenesis: a potential target for future therapeutics. Human Reproduction Update, 2018 Jan 1;24(1):59-85

Activin A mRNA is incresed by TNF-α in myometrial and leiomyoma cells

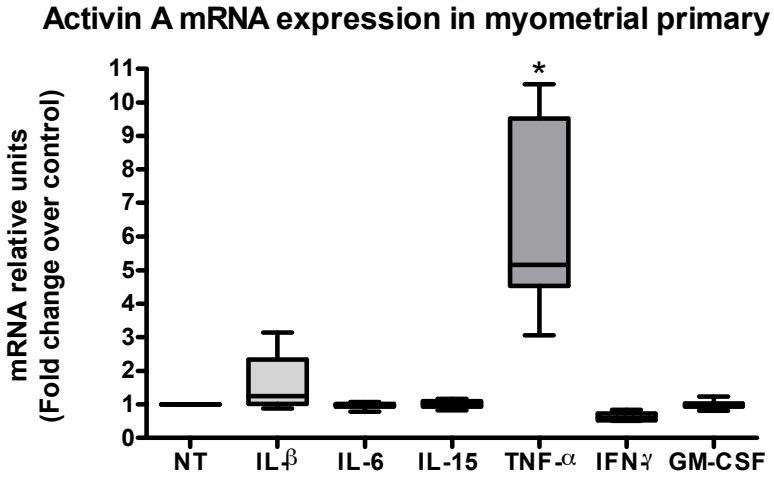

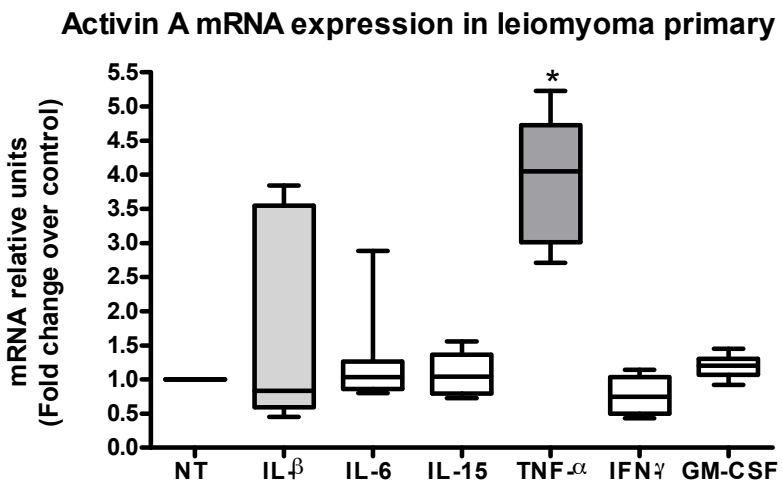

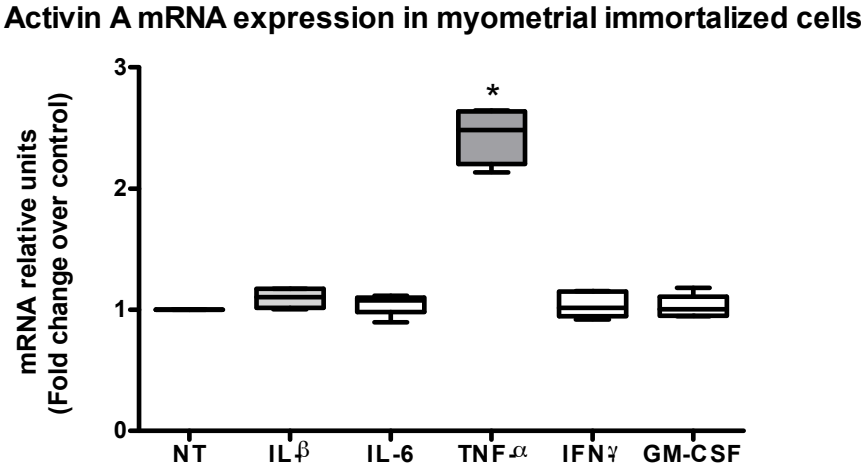

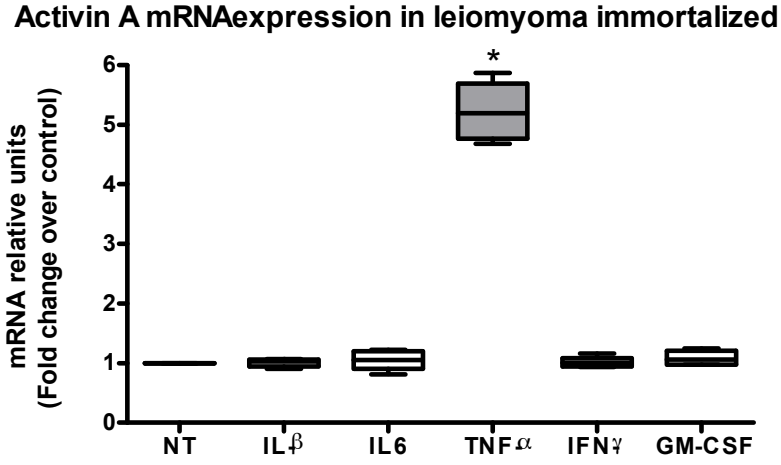

Real-time PCR showing the effect of inflammatory molecules on activin A subunit (INHBA) m RNA expression. A-B, primary cells (data from 3 different patients); C-D cell line (n=3) $P < 0.01$.

Protic O, Toti P, Islam MS, Occhini R, Giannubilo SR, Catherino WH, Cinti S, Petraglia F, Ciavattini A, Castellucci M, Hinz B, Ciarmela P. Possible involvement of inflammatory/reparative processes in the development of uterine fibroids. Cell Tissue Res. 2016 May;364(2):415-27

Higher numbers of macrophages were found inside and in the vicinity of leiomyoma as compared to the more distant surrounding myometrium.

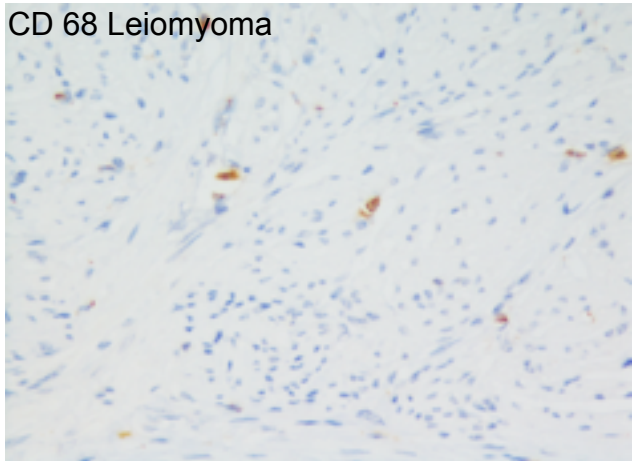

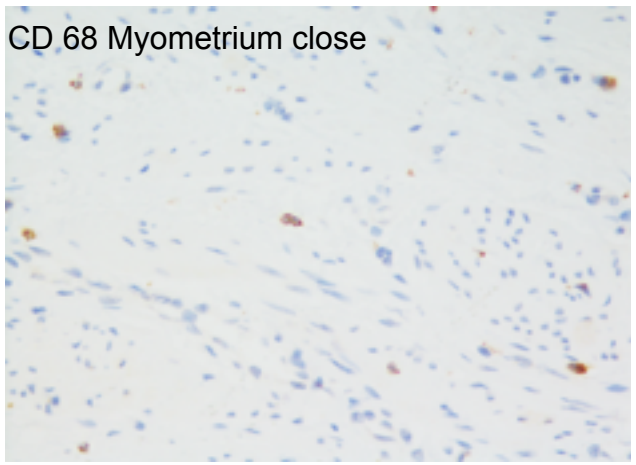

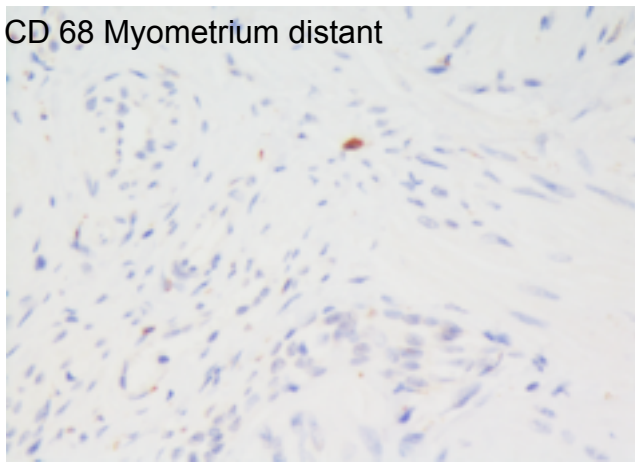

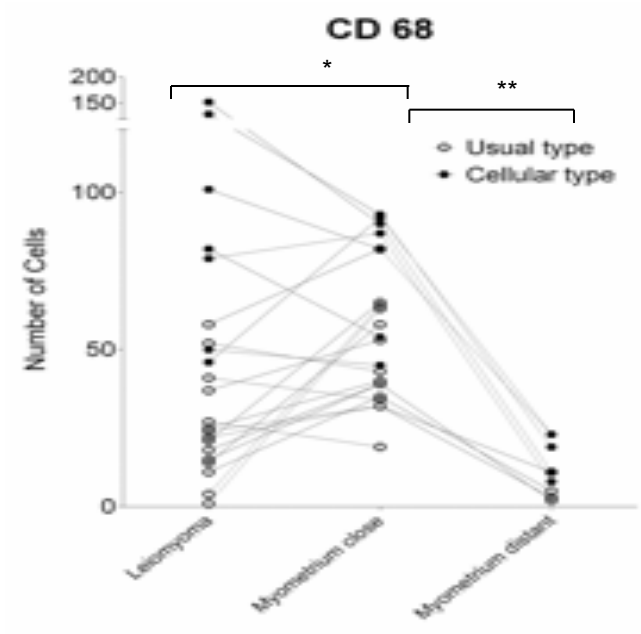

The total number of macrophages in five fields (corresponding to 0.17 mm^2), in leiomyoma, myometrium close and myometrium distant. Original magnification x400.

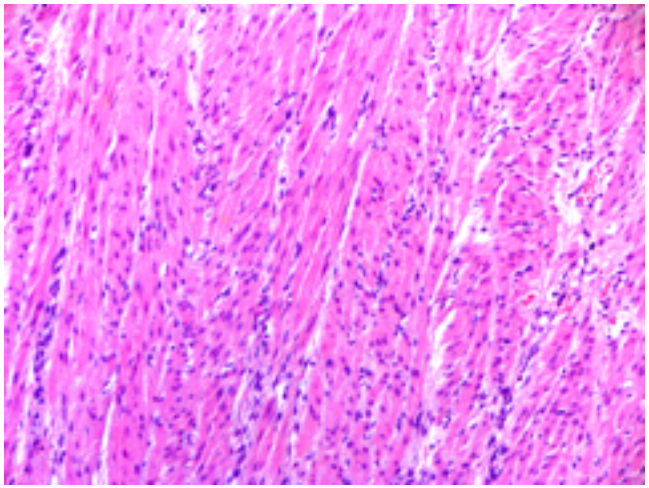

Normal myometrium

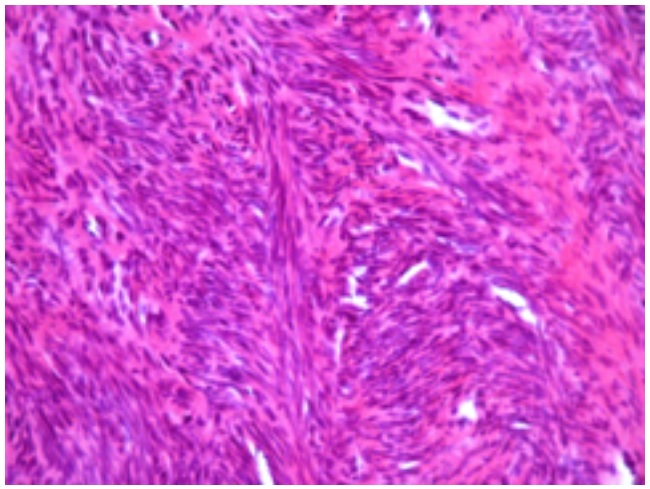

Usual leiomyoma

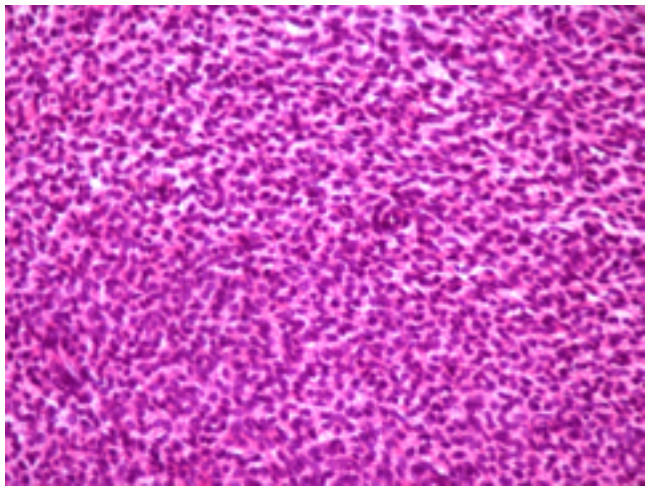

Cellular leiomyoma

Islam MS, Protic O, Giannubilo SR, Toti P, Tranquilli AL, Petraglia F, Castellucci M and Ciarmela P. Uterine leiomyoma: available medical treatments and new possible therapeutic options. J Clin Endocrinol Metab. 2013; 98(3): 921-34.

Cellular leiomyomas showed more macrophages and mast cells than the usual type

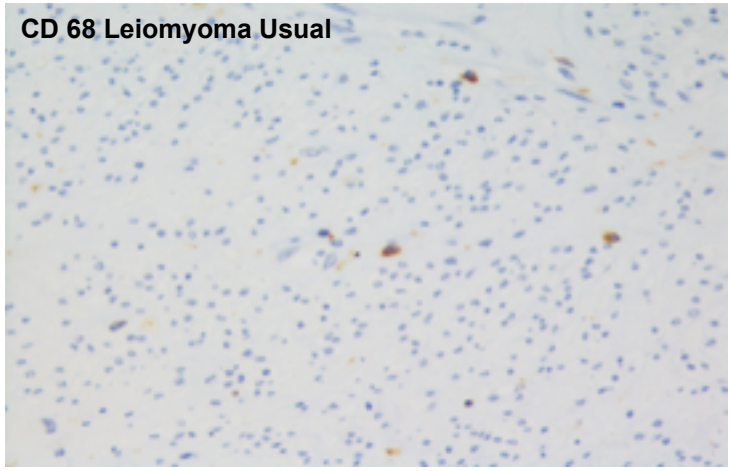

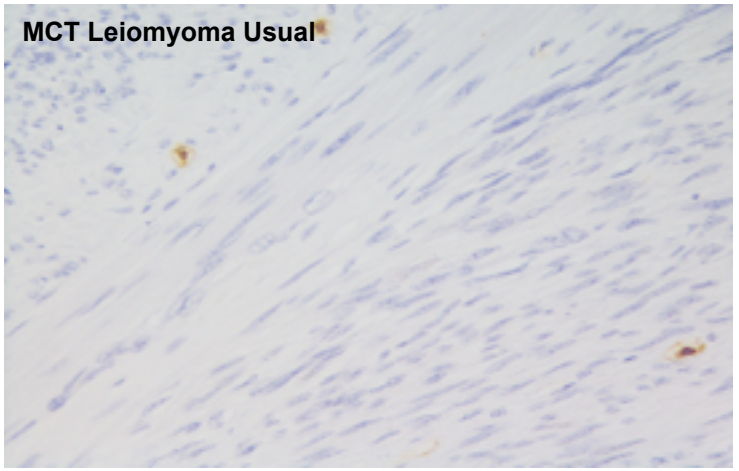

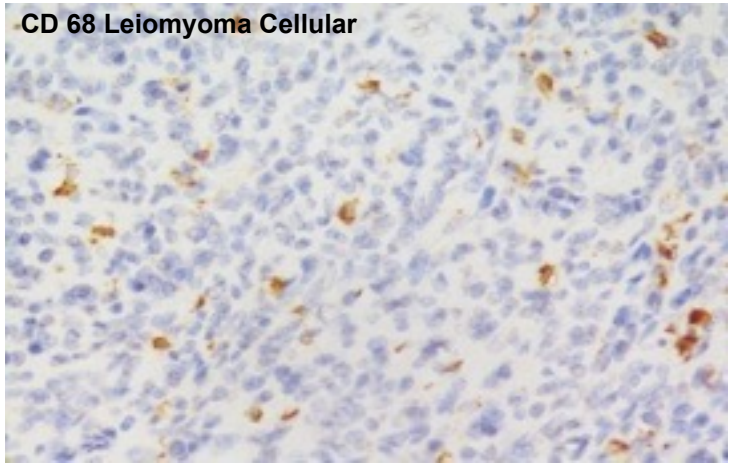

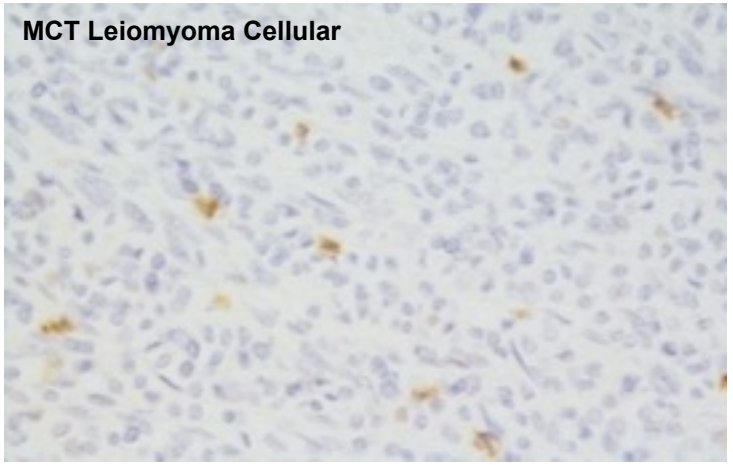

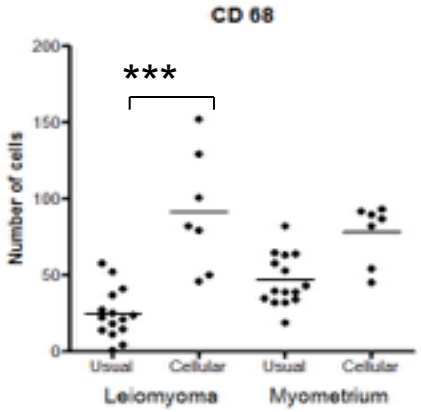

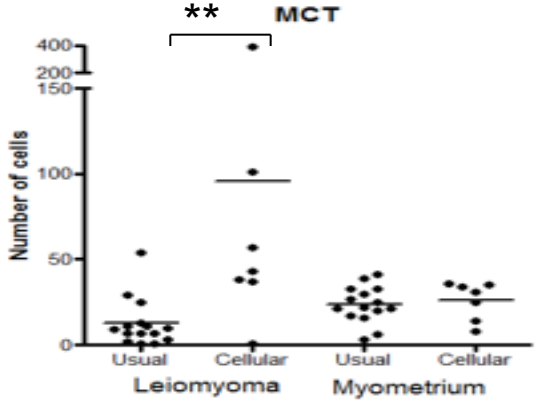

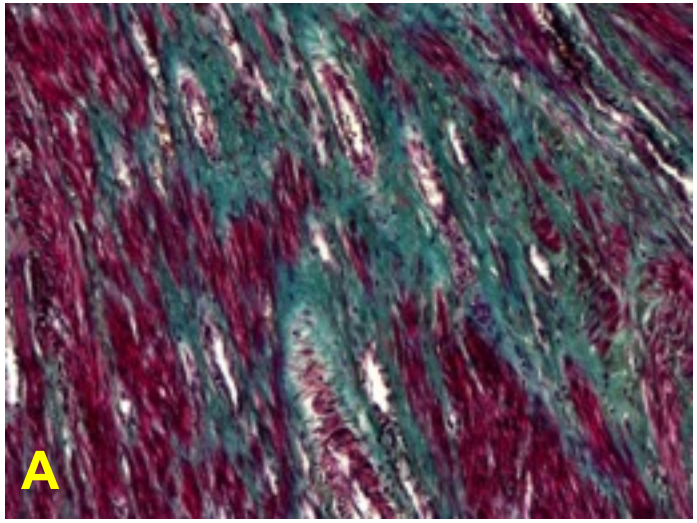

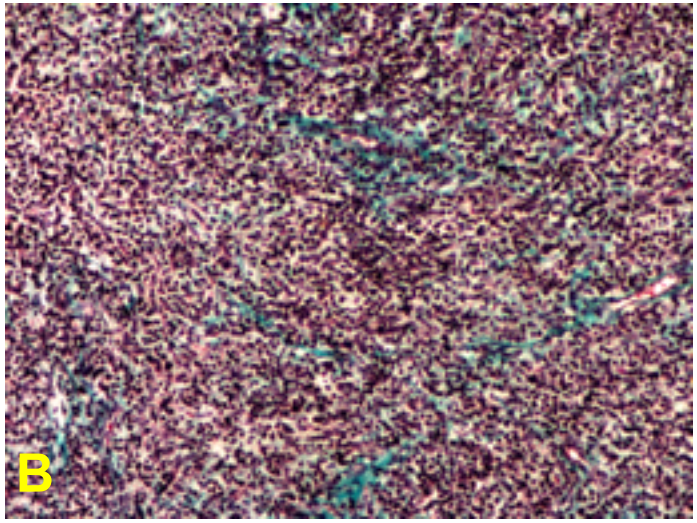

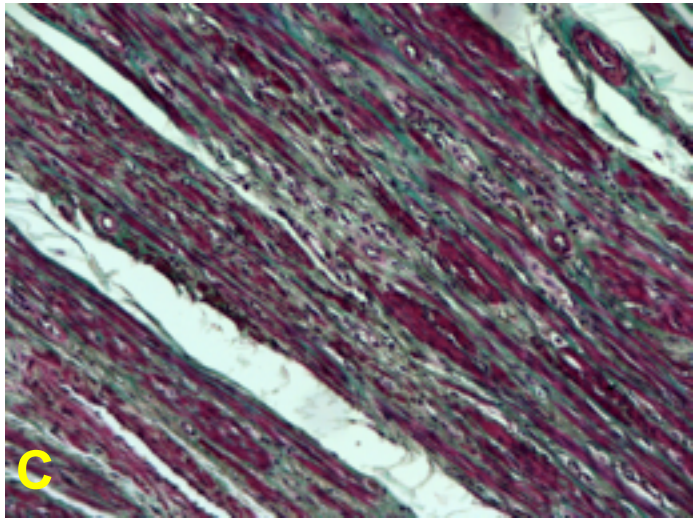

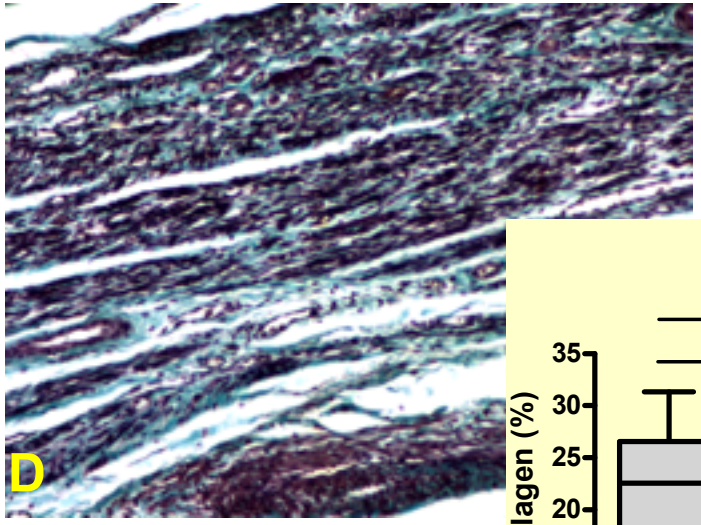

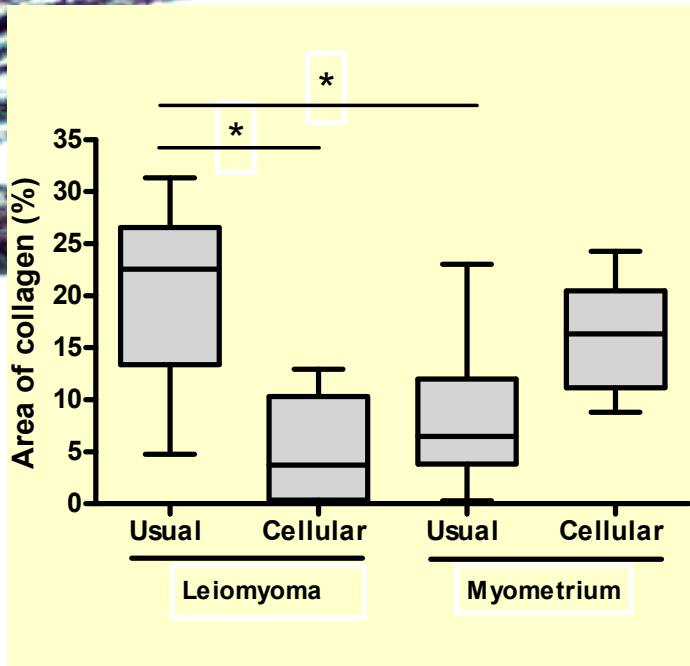

Figure 3. Collagen consistency and deposition in usual type (A), cellular type (B) of leiomyoma and corresponding myometrium of usual type (C) and cellular type (D) of leiomyoma. Masson's trichrome stain highlights green=collagen and red=smooth muscle. Original magnification x400. Evaluation of percentage of collagen present (E). The values are expressed as median (1st – 3rd quartiles).

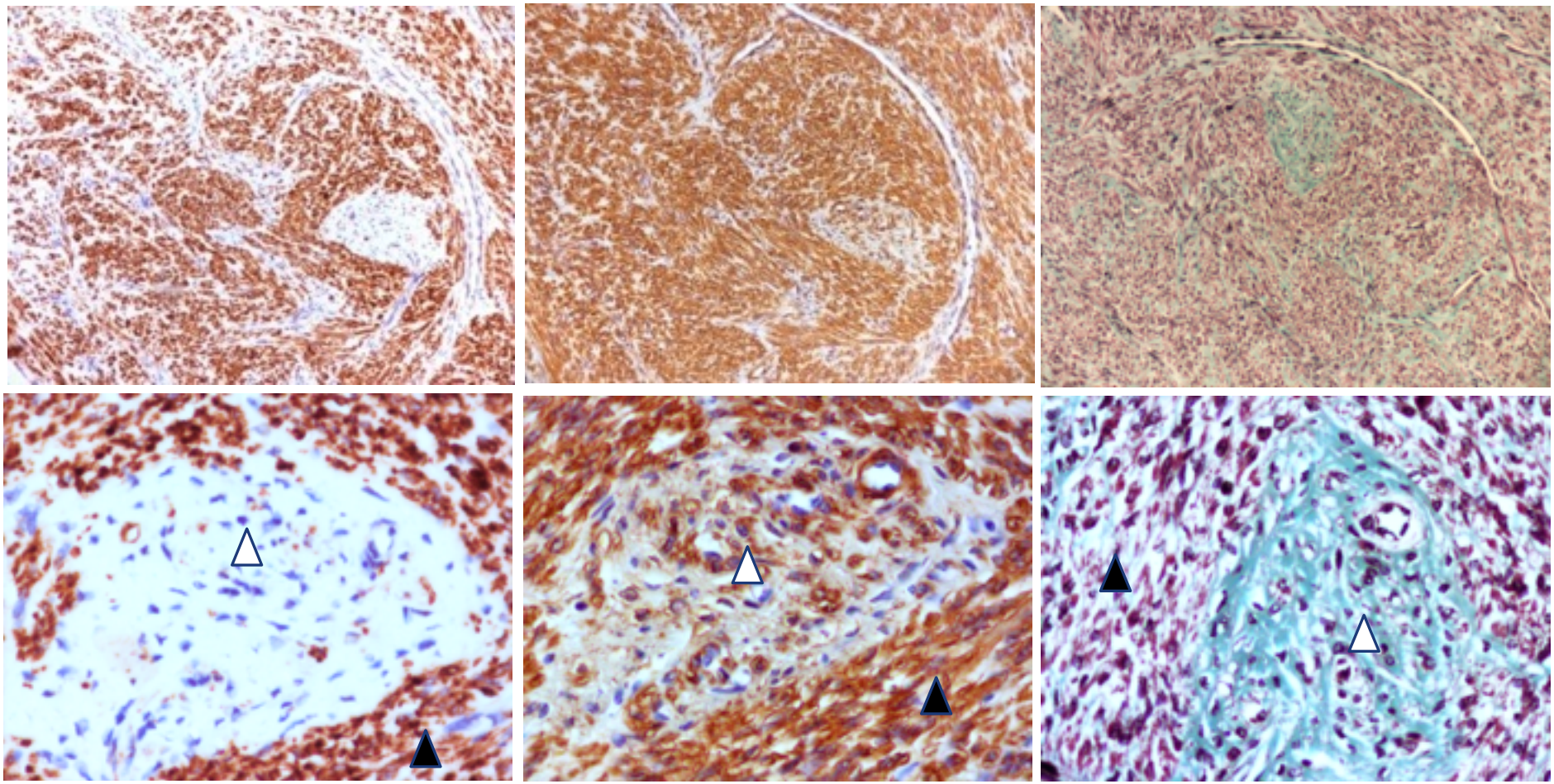

Immunohistochemical staining of Desmin, α-sma and Masson's Trichrome stain of serial sections of cellular type uterine leiomyoma tissue. The α-sma positive and desmin positive smooth muscle cells are pointed by the black arrowheads. The α-sma positive, desmin negative myofibroblasts closely associated to the presence of collagen are indicated by the white arrowheads. Original magnification x400.

Cells positive for α-sma, but negative for desmin and surrounded by a large amount of collagen are suggestive of myofibroblasts producing ECM

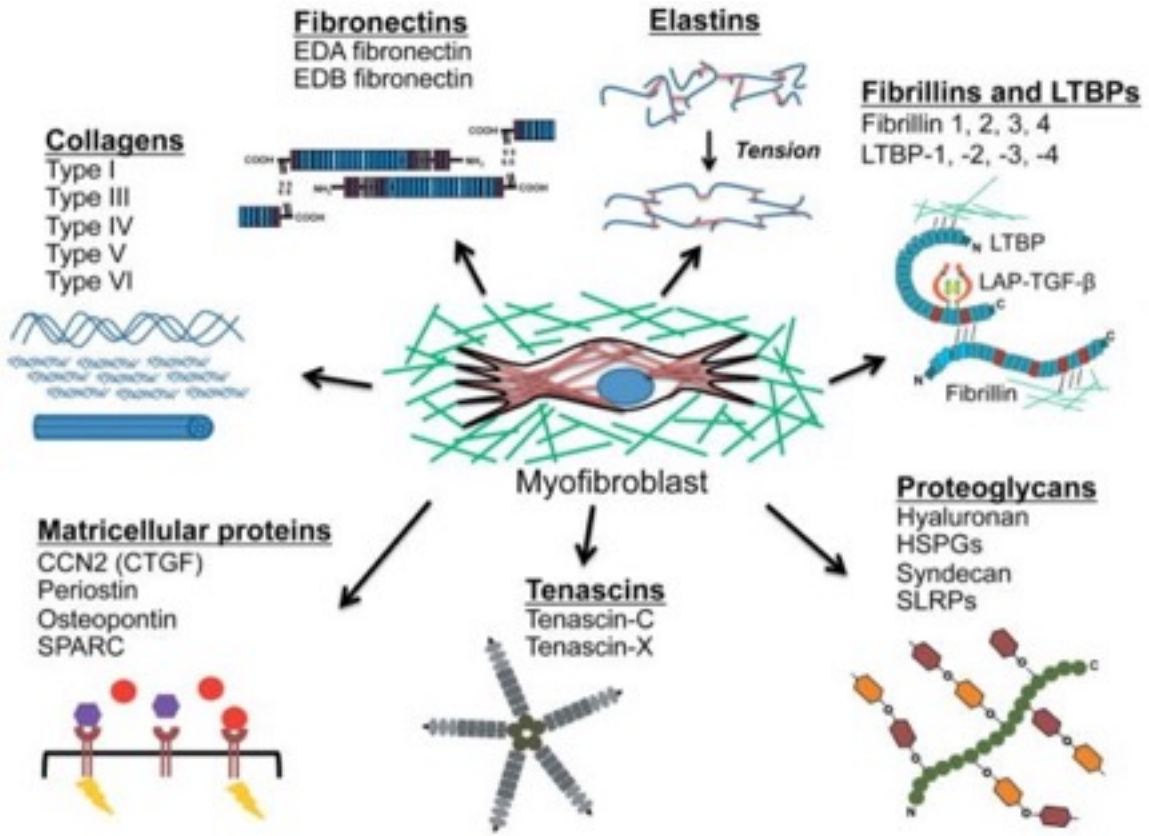

The myofibroblast matrix. Schematic of some of the ECM molecules relevant to tissue fibrosis. The myofibroblast (centre, with red stress fibres containing α-smooth muscle actin) lies enmeshed in its ECM (green). Components of the ECM are depicted (clockwise, from the 12 o'clock position): elastins, fibrillins and LTBPs, proteoglycans, tenascins, matricellular proteins, collagens, and fibronectins. The myofibroblast encounters, signals, and modulates the expression of these various components.

The myofibroblast matrix: implications for tissue repair and fibrosis. Klingberg F, Hinz B, White ES. J Pathol. 2013 Jan;229(2):298-309. doi: 10.1002/path.4104. Review.

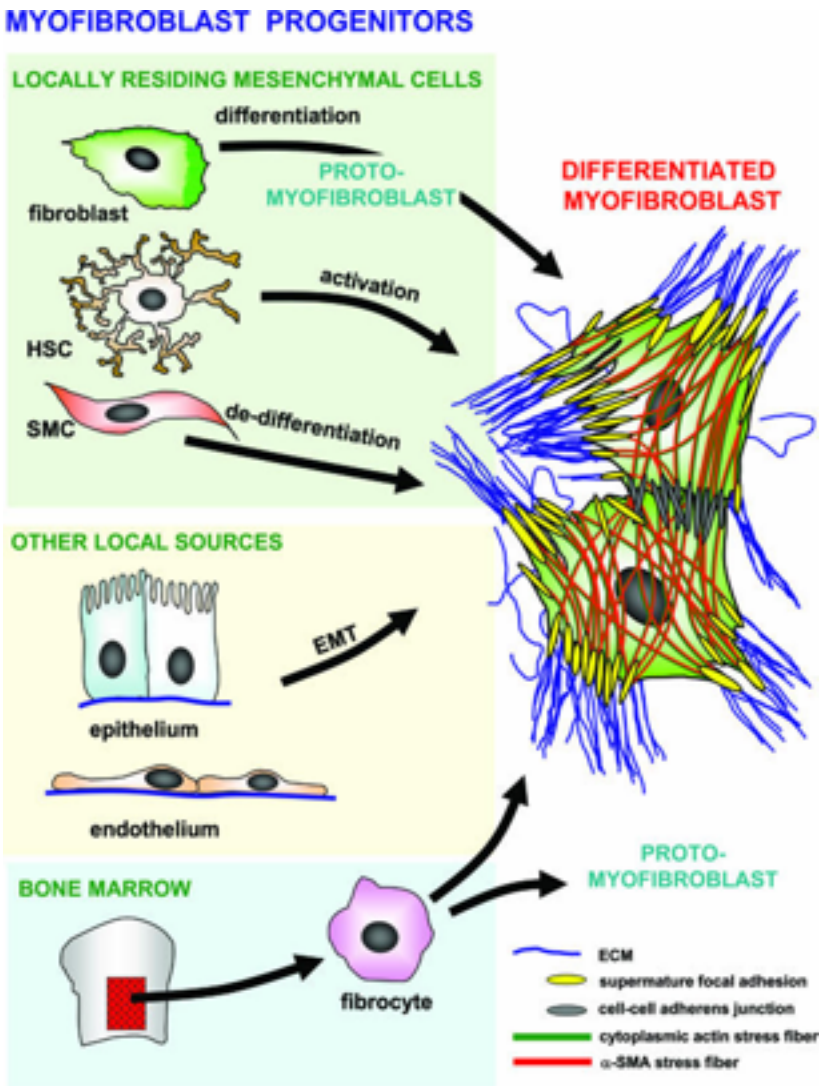

One cell, multiple origins. Differentiated myofibroblasts are characterized by increased production of ECM proteins and by the development of α-SMA-positive stress fibers that are connected with the ECM at sites of supermature FAs and between cells via adherens junctions. The main myofibroblast progenitor after injury of different tissues seems to be the locally residing fibroblast, which transiently differentiates into a protomyofibroblast, characterized by α-SMA-negative stress fibers. In the liver, myofibroblasts are additionally recruited from HSCs that follow an activation process and from epithelial cells that undergo EMT. In the lung, endothelial-to-mesenchymal transition may provide another mechanism to generate myofibroblasts. During atheromatous plaque formation, de-differentiating SMCs (ie, that lose late SMC markers) from the media are suggested to be the major source of myofibroblastic cells. The relative contribution of BM-derived circulating fibrocytes to the formation of differentiated myofibroblasts in different fibrotic lesions is unclear at present; it is conceivable that fibrocyte transdifferentiation terminates at the protomyofibroblast stage.

The myofibroblast: one function, multiple origins. Hinz B, Phan SH, Thannickal VJ, Galli A, Bochaton-Piallat ML, Gabbiani G. Am J Pathol. 2007;170:1807-16.
Review

ORIGINE OF MYOFIBROBLASTS

Fibroblastic cells expressing the trasmembrane cell surface glycoprotein, CD34, behave as mesenchymal stem cell progenitors and play an important role in wound healing and tissue repair.

When activated, these cells loose CD34 expression and may acquire α-sma expression, giving rise to myofibroblasts.

CD34 staining in myometrium and leiomyoma usual type

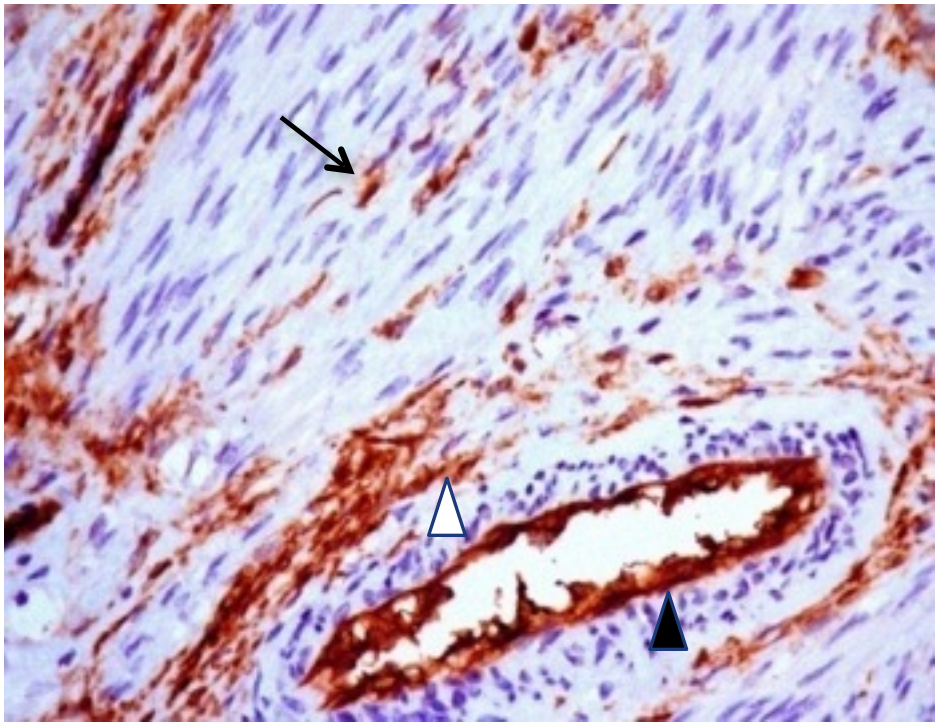

Based on the shape, location and intensity of the stain, we discriminated three different populations of CD34 positive cells: (i) vascular endothelial cells, indicated by black arrowhead; (ii) adventitial cells located in the outermost connective tissue layer of the large vessels, indicated by white arrowhead, especially in adventitia of the spiral arteries; and (iii) stromal fibroblastic cells, indicated by arrow, that appeared diffuse in the leiomyoma stroma, characterized by oval- slender nucleus and elongated multipolar cytoplasm.

Uterine leiomyoma CD34+/CD49+ cells exhibit characteristic of somatic stem/progenitor cells and are able to initiate tumors in vivo.

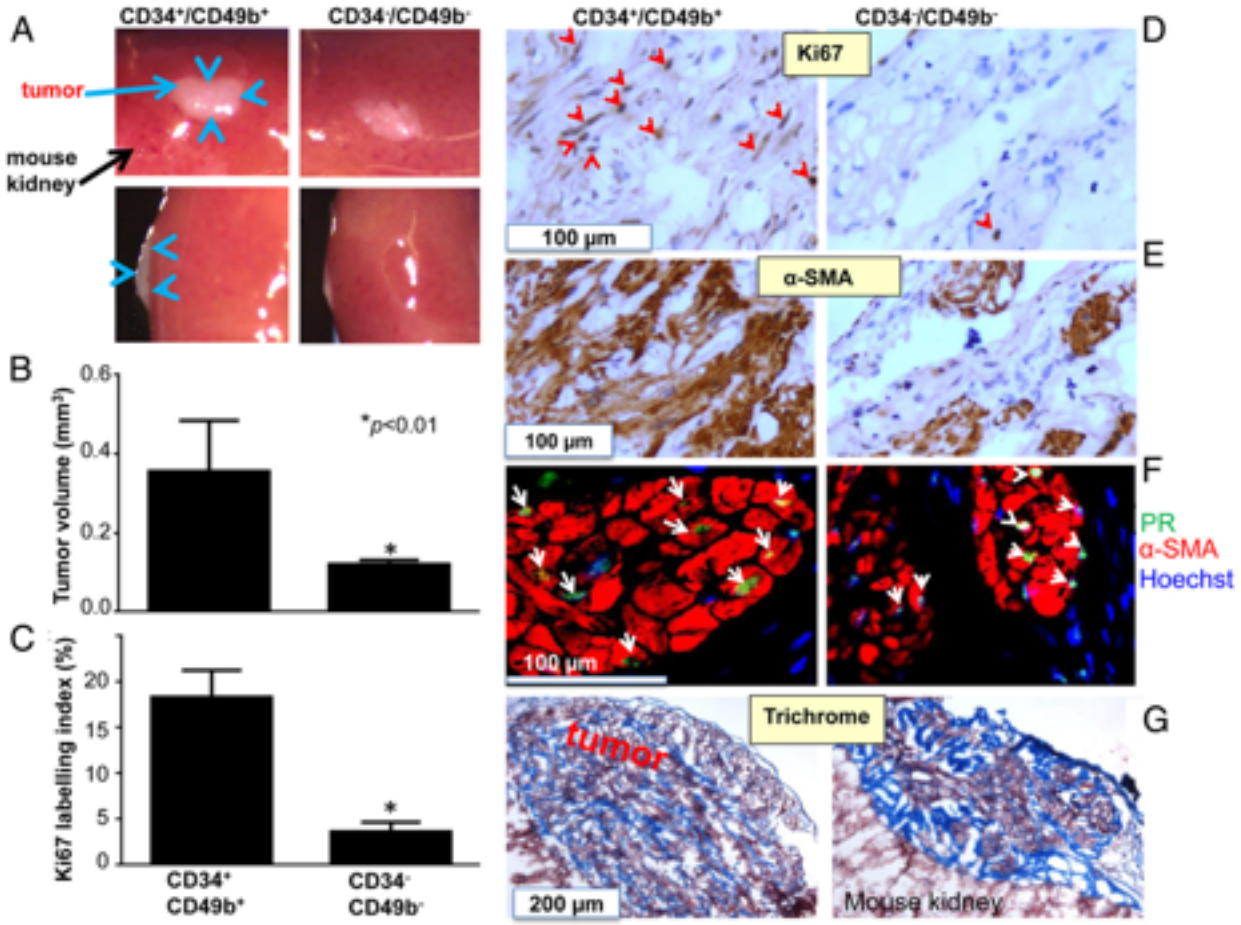

Figure 2. Regeneration of human leiomyoma-like tumors by CD34+/CD49b+ cells. A, Macroscopic visualization of the regenerated tumor (blue arrows) 8 weeks after engrafting. B, Quantification of tumor volume. Data shown are mean +/- SEM of representative triplicate experiments, repeated using cells from three independent patient samples. C, Quantification of the percentage of Ki67 positive cells (Ki67 labeling index) in tumors regenerated from CD34+/CD49b+ and CD34-/CD49b- cells. Values are expressed as means +/- SEM of representative triplicate experiments, repeated using cells from 3 patient samples. D–E, : Representative images of immunostaining of CD34+/CD49b+ or CD34-/CD49b- cell-reconstituted leiomyoma tissues with antibodies against proliferation marker Ki67 (D) and α-SMA (E). Tissues were counterstained with hematoxylin. Red arrowheads indicate Ki67-positive cells. F, Immunofluorscent staining of CD34+/CD49b+ or CD34-/CD49b- cell-reconstituted leiomyoma tissues with antibodies against PR (green) and α-SMA (red). Nuclei were stained with Hoechst dye (blue) and white arrowheads indicate PR-positive cells. G, Trichrome staining to characterize expression of typical extracellular matrix proteins in regenerated tissues.

Human Uterine Leiomyoma Stem/Progenitor Cells Expressing CD34 and CD49b Initiate Tumors In Vivo. Yin P, Ono M, Moravek MB, Coon JS 5th, Navarro A, Monsivais D, Dyson MT, Druschitz SA, Malpani SS, Serna VA, Qiang W, Chakravarti D, Kim JJ, Bulun SE. J Clin Endocrinol Metab. 2015 Apr;100(4):E601-6

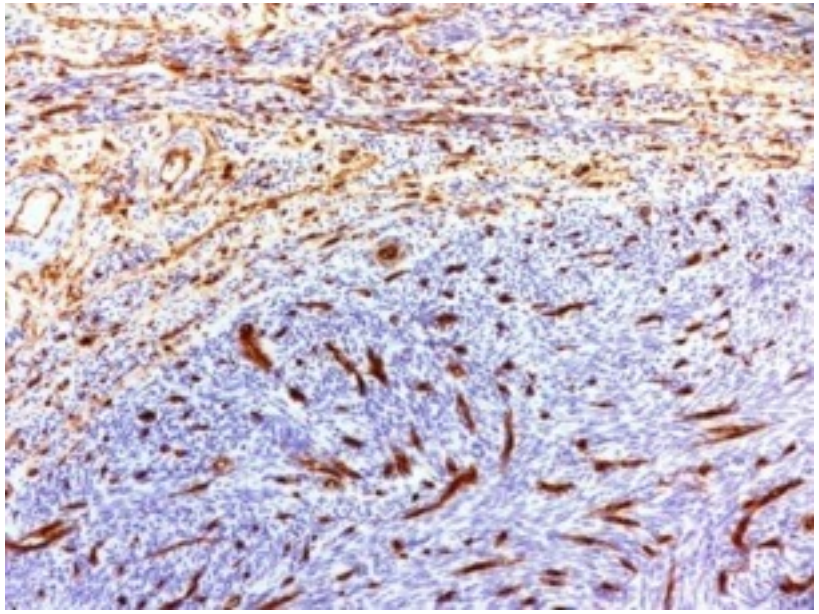

Very small (less than 0,5 cm) leiomyoma, that were probably developing leiomyoma.
There were no CD34 positive stromal fibroblasts. The CD34 positivity was restricted to vascular endothelial cells.

In cellular type leiomyoma there were no CD34 positive stromal fibroblasts. The CD34 positivity was restricted to vascular endothelial cells.

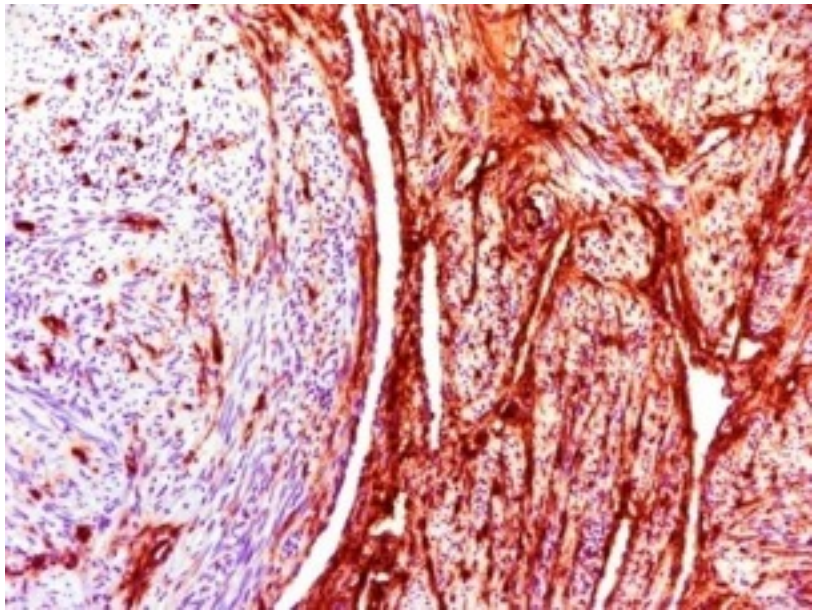

Are the mesenchymal stem cell progenitors activated to give origine to myofibroblasts?

It may possible that the leiomyoma cellular type is a first step in the leiomyoma formation rather that a distict hystological type.

Protic O, Toti P, Islam MS, Occhini R, Giannubilo SR, Catherino WH, Cinti S, Petraglia F, Ciavattini A, Castellucci M, Hinz B, Ciarmela P. Possible involvement of inflammatory/reparative processes in the development of uterine fibroids. Cell Tissue Res. 2016 May;364(2):415-27

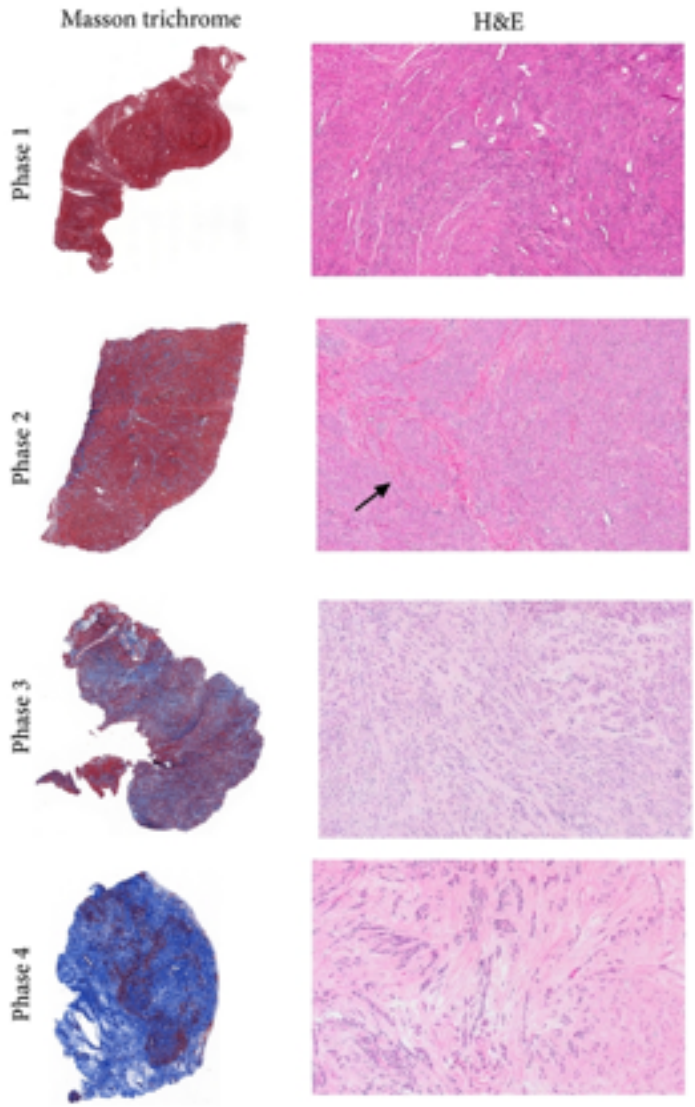

Fibroid Phases 1–4. Representative examples of the four phases of fibroid development are shown, with the Masson trichrome stain (1x image) on the left and the H&E stain of the same tumor (10x image) on the right. The progressive increase in blue staining collagen from Phase 1 to Phase 4 is well shown in the Masson trichrome stained sections. The corresponding H&E images on the right also demonstrate the virtual absence of collagen in the Phase 1 tumor, the appearance of interspersed pink collagenous fibers (arrow) in Phase 2, the more abundant pale pink collagenous stroma of Phase 3, and the predominance of pink, hyalinized stroma in Phase 4. Note also the abundance of microvessels (small ovoid spaces) in Phase 1 and the paucity of vessels in Phases 3 and 4.

The natural history of uterine leiomyomas: light and electron microscopic studies of fibroid phases, interstitial ischemia, inanosis, and reclamation. Flake GP, Moore AB, Sutton D, Kissling GE, Horton J, Wicker B, Walmer D, Robboy SJ, Dixon D. Obstet Gynecol Int. 2013;2013:528376

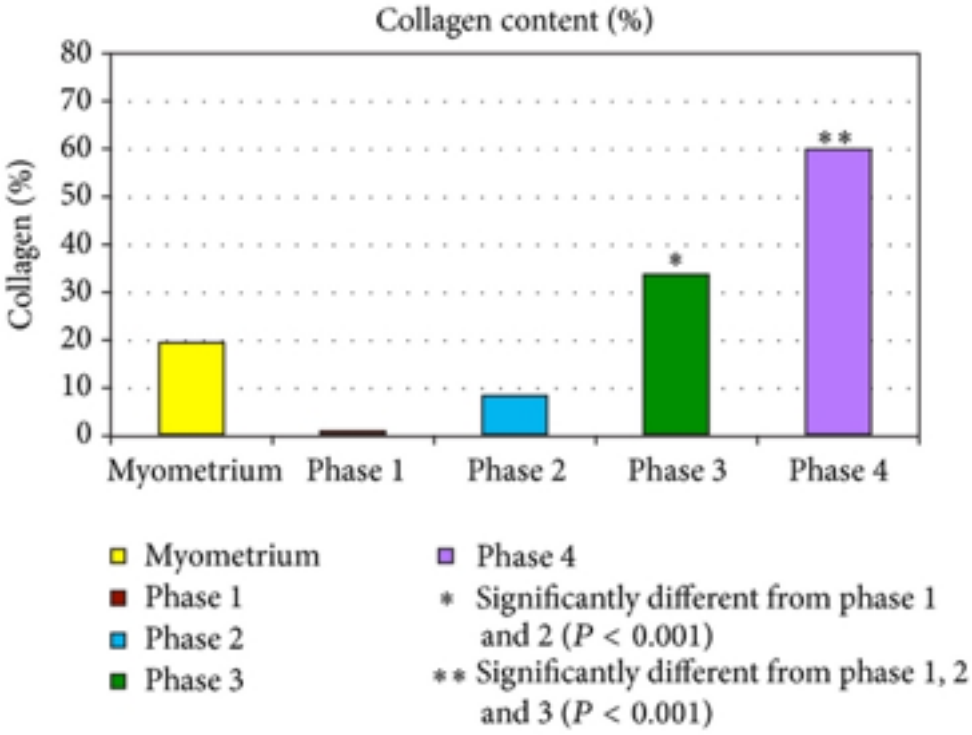

Mean percent collagen content of fibroid phases 1–4 by image analysis. The bar graph depicts the progressive accumulation of collagen in the transition from phase 1 to 4. There were 5 samples per phase group and the values represent the means. The myometrial bar is the mean value of 8 samples. Significantly different from phases 1 and 2 (). Significantly different from phases 1, 2 or 3 ().

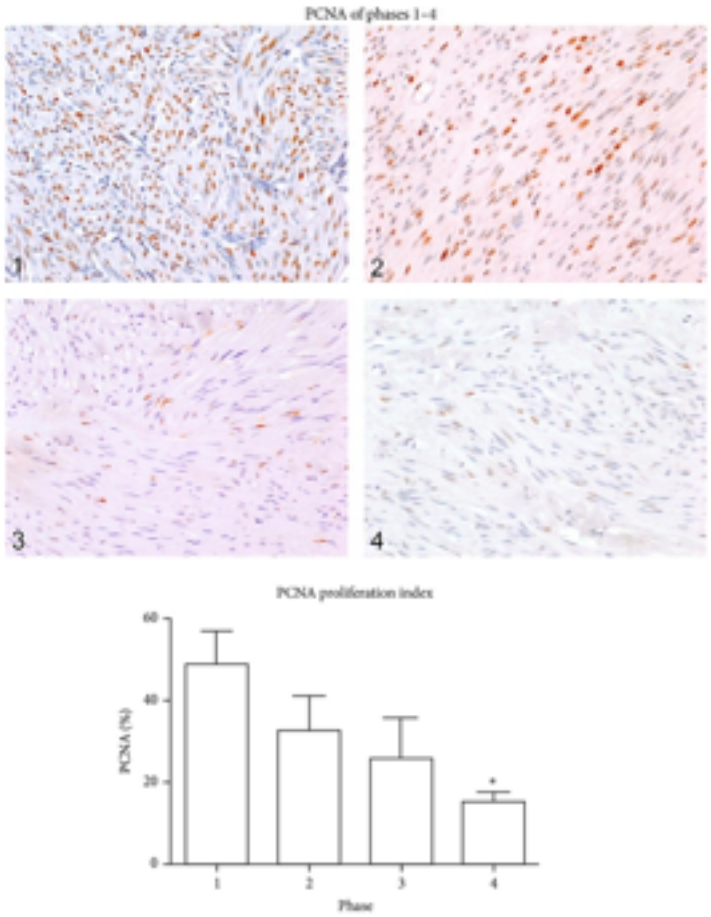

Fibroid phases: comparison of PCNA staining. (a) In this panel, a representative image of PCNA immunostaining from a fibroid in each of the four phases is shown. The percentage of PCNA positive nuclei in areas of maximum staining within the 4 fibroids in this panel was 59.1, 25.3, 19.1, and 15.5 for phases 1, 2, 3, and 4, respectively. A few PCNA positive nuclei are present in the phase 4 photo, but these are less intensely stained and thus less obvious than those in the other phases. All images were taken with the 20x objective. (b) Bar graph of Mean PCNAs from each phase

The natural history of uterine leiomyomas: morphometric concordance with concepts of interstitial ischemia and inanosis. Flake GP, Moore AB, Flagler N, Wicker B, Clayton N, Kissling GE, Robboy SJ, Dixon D. Obstet Gynecol Int. 2013;2013:285103

We suggest inflammatory/reparative pathogenesis:

The increase of inflammatory cells may trigger fibrotic process with recruitment of stem cells that give origine to myofibroblasts expressing abnormal ECM.

Mechanotransduction of extracellular matrix in uterine leiomyoma

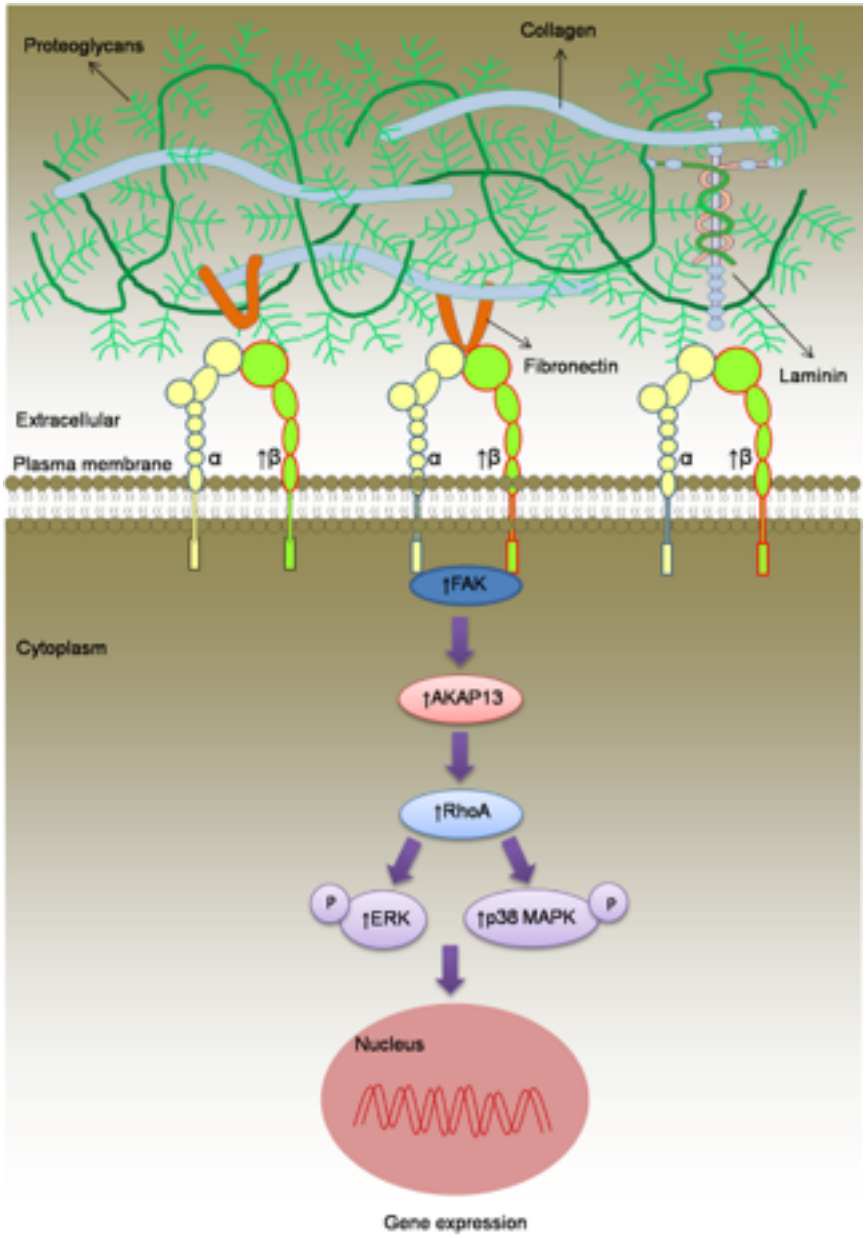

Islam MS, Ciavattini A, Petraglia F, Castellucci M, Ciarmela P. Extracellular matrix in uterine leiomyoma pathogenesis: a potential target for future therapeutics. Hum Reprod Update. 2018 Jan 1;24(1):59-85

Cell Membrane & Extracellular Matrix

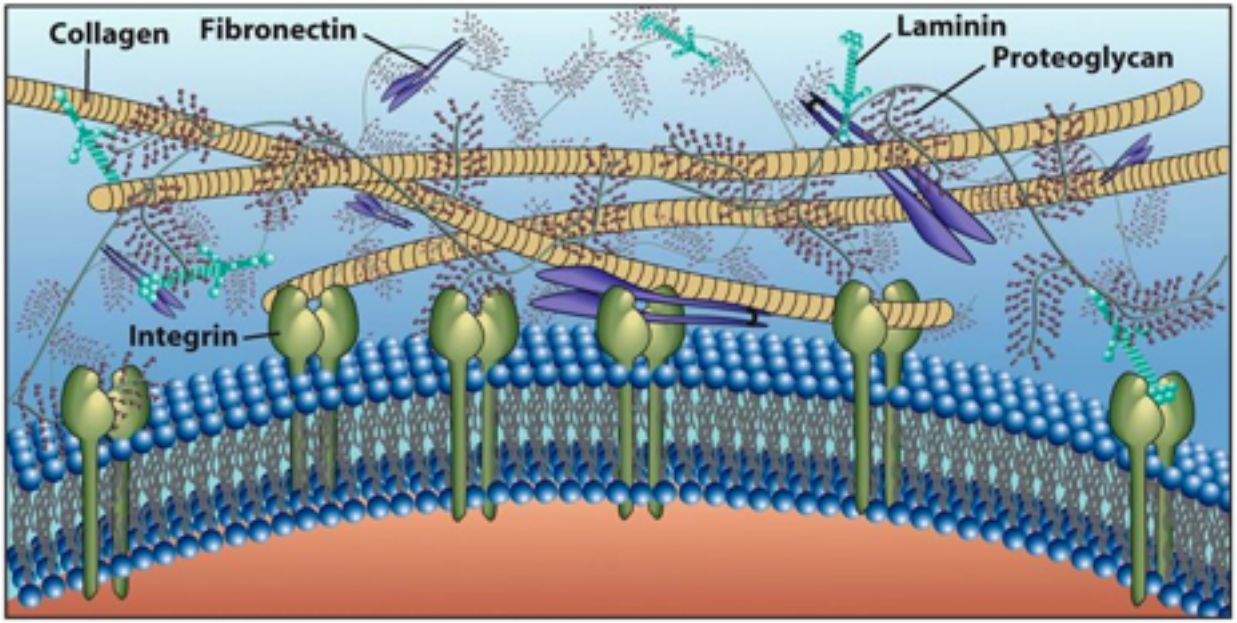

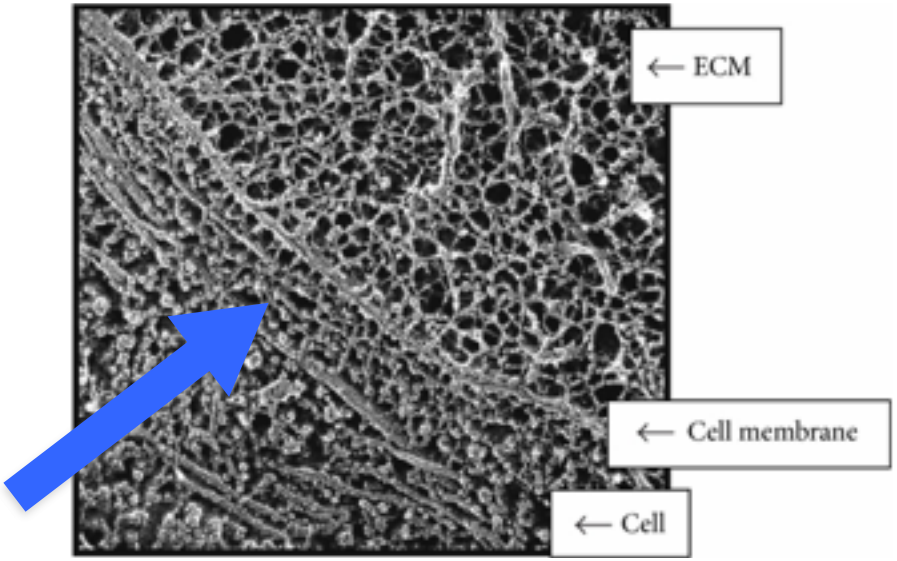

Omega-3 Fatty Acids

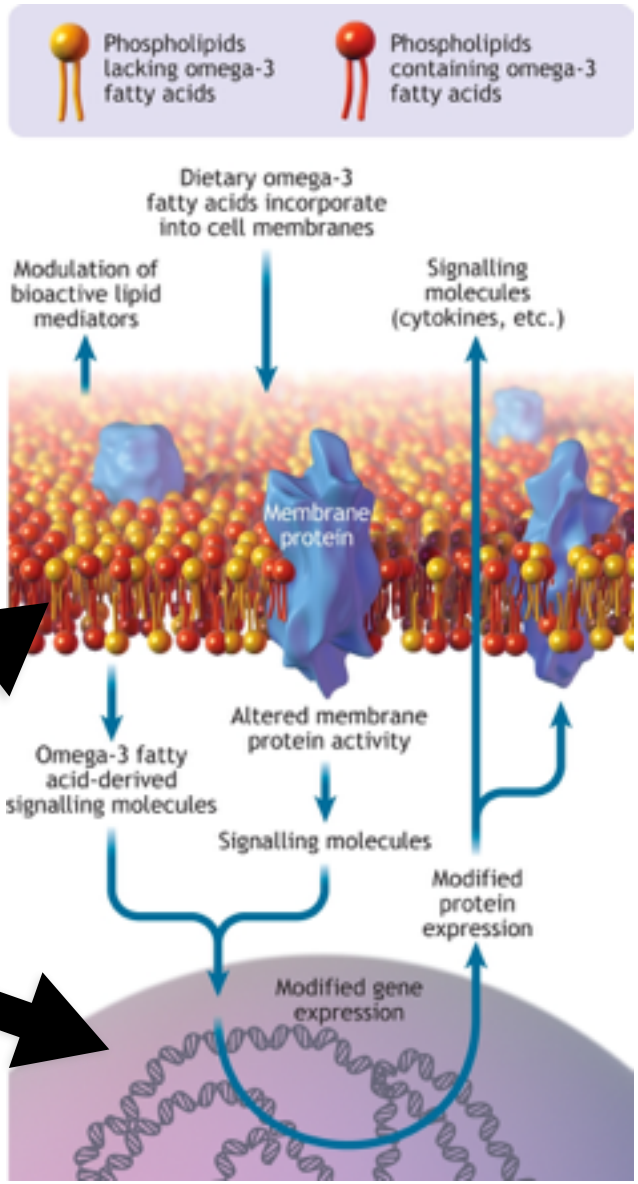

Polyunsaturated fatty acids (PUFA)

Eicosapentaenoic acid

Docosahexaenoic acid

Primary leiomyoma and myometrial tissue

Cell cultures treated with EPA and DHA

Transmethylation of tissue fatty acids

Gaschromatographic analysis of fatty acid content

To analyze if omega-3 fatty acids modulate the lipidomic profile of the cell.

Laurdan fluorescence for membrane fluidity or rigidity

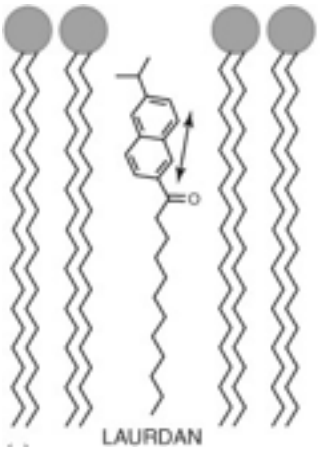

To assess the effects of omega-3 fatty acids on the fluidity of the cell membrane.

Real-time PCR for gene expression

ECM components

Mechanical signaling

Sterol regulatory molecules

Mitochondrial enzymes

In vitro effect of DHA and EPA on fatty acid composition in Myometrial cells

Fatty acids		Myo_ctrl	Myo_DHA	Myo_EPA
Name	*Carbon number: double bond number*	*weight % of total fatty acids*		
Myristic acid	14:0	2.4±0.7	2.5±0.5	2.6±0.5
Pentadecylic acid	15:0	1.3±0.2	1.1±0.2	1.1±0.2
Palmitic acid	16:0	19.9±2.3	21.8±2.1	21.1±1.4
Margaric acid	17:0	0.9±0.1	0.8±0.1	0.8±0.1
Stearic acid	18:0	18.0±2.8	19.7±2.4	18.5±2.4
Lignoceric acid	24:0	1.1±0.3^{b}	0.7±0.1^{a}	0.8±0.1^{a}
	∑SFA	**43.5±5.3**	**46.6±4.1**	**44.9±2.9**
Pentadecenoic acid	15:1	1.0±0.8	0.8±0.5	0.8±0.4
Palmitoleic acid	16:1 *n*-7	5.7±0.5^{b}	4.3±0.6^{a}	4.2±0.7^{a}
Heptadecenoic acid	17:1	0.6±0.4	0.4±0.3	0.3±0.3
Oleic acid	18:1 *n*-9	25.6±2.0^{b}	18.6±3.0^{a}	17.9±2.7^{a}
Vaccenic acid	18:1 *n*-7	8.9±2.3^{b}	6.7±1.9^{ab}	6.4±1.6^{a}
Nervonic acid	24:1	0.3±0.1^{b}	0.1±0.0^{a}	0.1±0.0^{a}
	∑MUFA	**42.1±1.1^{b}**	**30.8±4.9^{a}**	**29.7±4.7^{a}**
Linoleic acid	18:2 *n*-6 cis	1.0±0.4^{a}	1.6±0.3^{b}	1.6±0.3^{b}
γ-Linolenic acid	18:3 *n*-6	0.0±0.0	0.1±0.0	0.1±0.1
α-Linolenic acid	18:3 *n*-3	0.1±0.1	0.1±0.0	0.1±0.0
Stearidonic acid	18:4 *n*-3	0.4±0.1^{b}	0.2±0.0^{a}	0.1±0.0^{a}
Eicosadienoic acid	20:2 *n*-6	0.1±0.1	0.1±0.0	0.1±0.0
Dihomo-γ-linolenic acid	20:3 *n*-6	1.1±0.2	1.2±0.3	1.1±0.2
Arachidonic acid	20:4 *n*-6	5.2±1.5^{b}	3.4±0.6^{a}	3.4±0.6^{a}
Eicosapentaenoic acid	20:5 *n*-3, EPA	0.3±0.2^{a}	1.2±0.8^{a}	5.1±2.2^{b}
Docosapentaenoic acid	22:5 *n*-3, DPA	1.7±0.9^{a}	2.2±1.1^{a}	10.5±3.4^{b}
Docosahexaenoic acid	22:6 *n*-3, DHA	2.3±1.2^{a}	11.0±5.6^{b}	1.4±0.8^{a}
	∑PUFA	**12.3±4.3^{a}**	**21.0±8.4^{ab}**	**23.7±7.0^{b}**
	∑PUFA ω3	4.8±2.3^{a}	14.7±7.3^{b}	17.4±6.0^{b}
	∑PUFA ω6	7.5±2.1	6.3±1.1	6.4±1.0
	Lipophilic index	30.8±5.0	27.1±7.0	23.2±5.9
	Other peaks	2.0±0.2	1.6±0.2	1.7±0.3

Omega-3 fatty acids modulate the lipid profile of the cell membrane

In vitro effect of DHA and EPA on fatty acid composition in Leiomyoma cells

		Fib_ctrl	Fib_DHA	Fib_EPA
Name	*Carbon number: double bond number*	*weight % of total fatty acids*		
Myristic acid	14:0	2.1±0.5	2.3±0.6	2.5±0.7
Pentadecylic acid	15:0	1.7±0.5	1.5±0.3	1.5±0.6
Palmitic acid	16:0	20.3±1.9	20.9±2.8	20.8±2.1
Margaric acid	17:0	0.7±0.1	0.8±0.1	0.8±0.1
Stearic acid	18:0	18.3±3.3	19.9±2.2	18.7±1.6
Lignoceric acid	24:0	1.1±0.3^{b}	0.7±0.2^{a}	0.8±0.2^{a}
	∑SFA	**44.2±5.5**	**46.1±5.2**	**45.1±3.4**
Pentadecenoic acid	15:1	0.9±0.4	1.3±0.7	1.5±0.8
Palmitoleic acid	16:1 *n*-7	6.5±1.0^{b}	4.9±0.6^{a}	4.9±0.8^{a}
Heptadecenoic acid	17:1	0.2±0.2	0.4±0.3	0.4±0.3
Oleic acid	18:1 *n*-9	24.0±2.3^{b}	19.0±0.6^{a}	18.9±0.4^{a}
Vaccenic acid	18:1 *n*-7	9.2±0.6^{b}	6.5±0.5^{ab}	6.4±0.5^{a}
Nervonic acid	24:1	0.2±0.1^{b}	0.1±0.0^{a}	0.1±0.0^{a}
	∑MUFA	**41.0±3.5^{b}**	**32.1±0.4^{a}**	**32.1±1.3^{a}**
Linoleic acid	18:2 *n*-6 cis	1.0±0.2^{a}	1.5±0.1^{b}	1.5±0.2^{b}
γ-Linolenic acid	18:3 *n*-6	0.1±0.0	0.0±0.0	0.1±0.0
α-Linolenic acid	18:3 *n*-3	0.1±0.0	0.1±0.0	0.1±0.0
Stearidonic acid	18:4 *n*-3	0.3±0.2^{b}	0.1±0.0^{a}	0.1±0.0^{a}
Eicosadienoic acid	20:2 *n*-6	0.1±0.0	0.2±0.2	0.1±0.0
Dihomo-γ-linolenic acid	20:3 *n*-6	1.1±0.3	1.2±0.1	1.1±0.1
Arachidonic acid	20:4 *n*-6	6.6±1.9^{b}	4.6±1.8^{a}	4.0±0.8^{a}
Eicosapentaenoic acid	20:5 *n*-3, EPA	0.3±0.1^{a}	1.5±0.7^{a}	5.3±1.8^{b}
Docosapentaenoic acid	22:5 *n*-3, DPA	1.6±0.9^{a}	1.6±0.9^{a}	7.0±0.9^{b}
Docosahexaenoic acid	22:6 *n*-3, DHA	1.8±1.1^{a}	9.4±2.9^{b}	1.3±1.0^{a}
	∑PUFA	**12.9±2.6^{a}**	**20.3±4.9^{ab}**	**20.7±2.1^{b}**
	∑PUFA ω3	4.1±2.2^{a}	12.8±4.2^{b}	13.9±2.0^{b}
	∑PUFA ω6	8.8±1.9	7.5±1.9	6.8±0.8
	Lipophilic index	30.5±4.2	27.2±5.7	25.4±3.1
	Other peaks	1.8±0.4	1.5±0.4	1.7±0.2

The **reduction of the arachidonic acid** suggests an **anti-inflammatory effect** of EPA and DHA on myometrial and leiomyoma cells.

Effects of EPA and DHA on membrane phase myometrial and leiomyoma cells

Primary myometrial cells

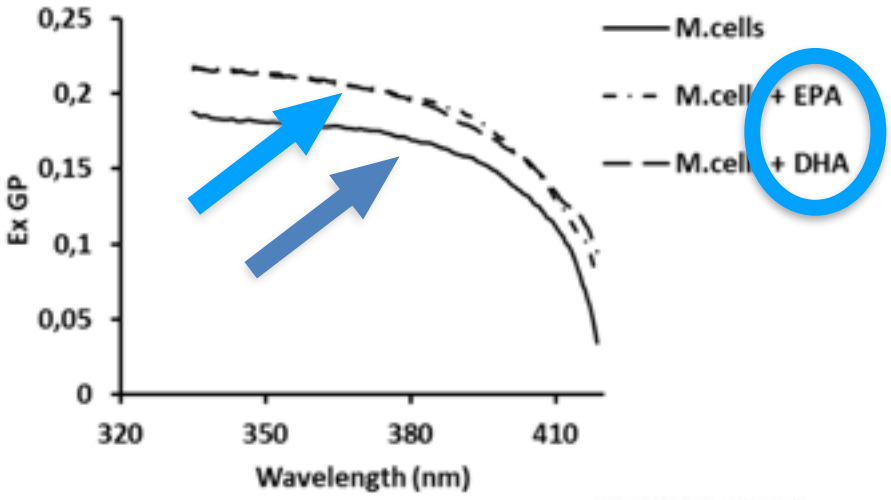

Primary leiomyoma cells

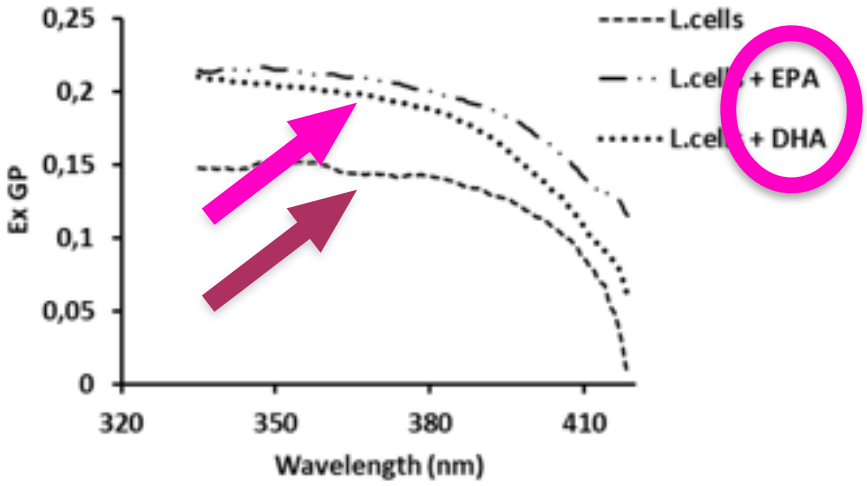

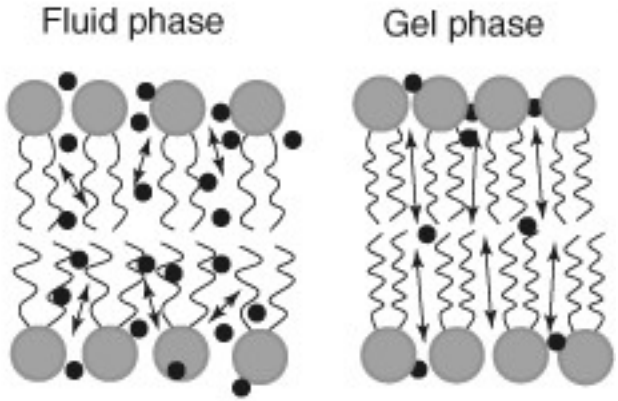

By using Laurdan Ex GP spectra we could identify that the membrane myometrial and leiomyoma cells were in the liquid-crystalline phase. Evaluation of both cell types after treatment with EPA or DHA showed that the Laurdan Ex GP values were increased compared to the control group, suggesting that the samples were in a more rigid environment with a decreased capacity of mobility due to a lower fluidity level of the membrane.

Effect of EPA and DHA on mRNA expression of extracellular matrix components and activin A in primary myometrial and leiomyoma cells

Primary myometrial cells

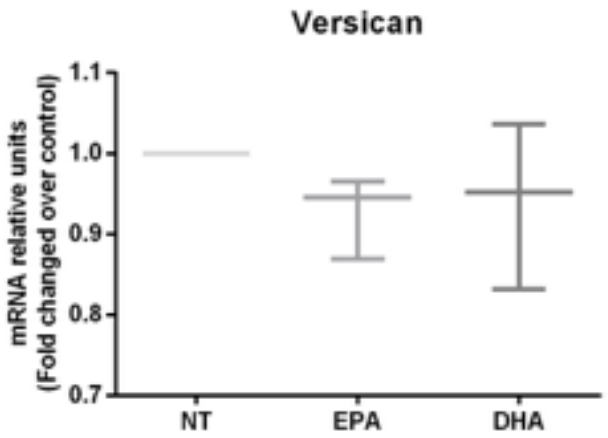

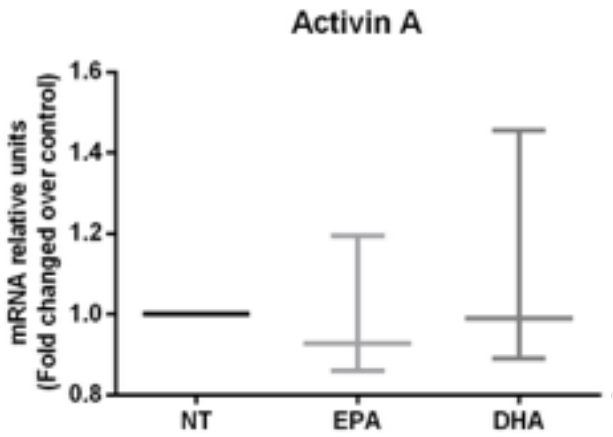

Primary leiomyoma cells

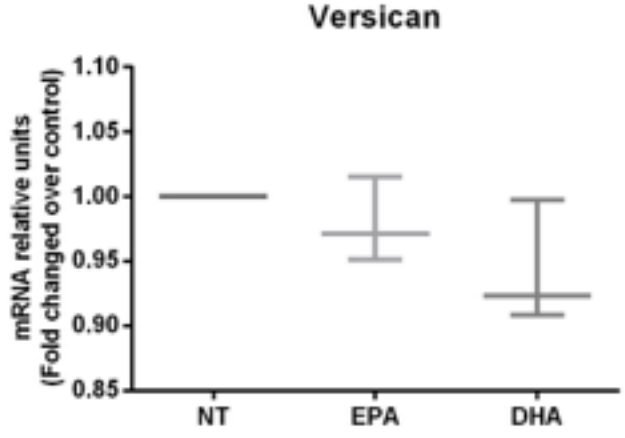

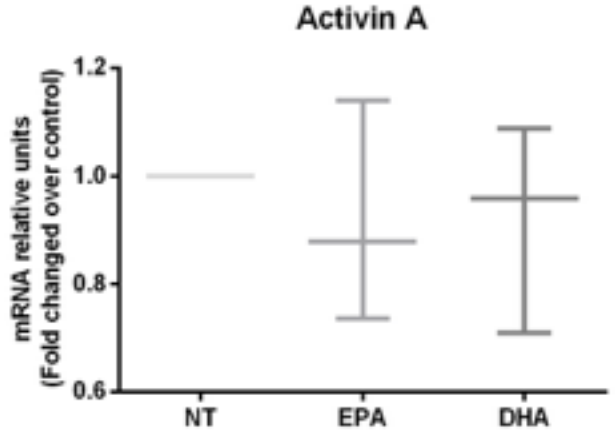

Cells of the myometrium or leiomyomas were treated with EPA or DHA (50 μM for 48 hours) and showed no significant changes of collagen1A1, fibronectin and versican and activin A mRNA expression compared to the untreated sample.

Effect of EPA and DHA on mRNA expression of mechanical signaling molecules in primary myometrial and leiomyoma cells

Primary myometrial cells

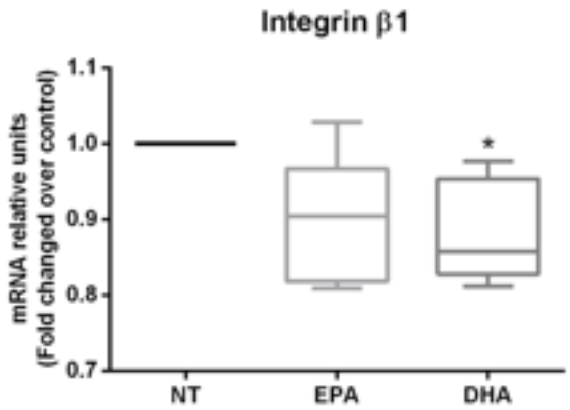

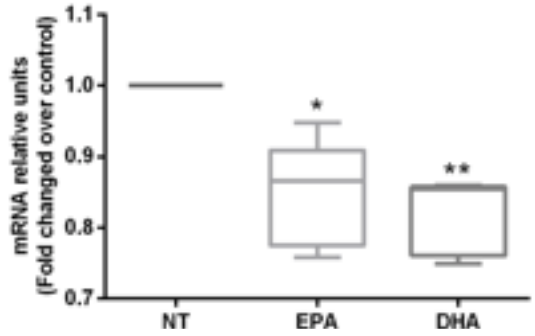

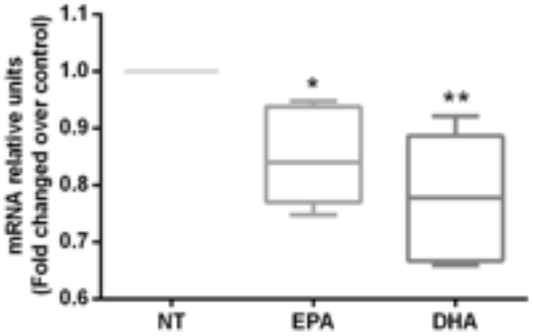

Primary leiomyoma cells

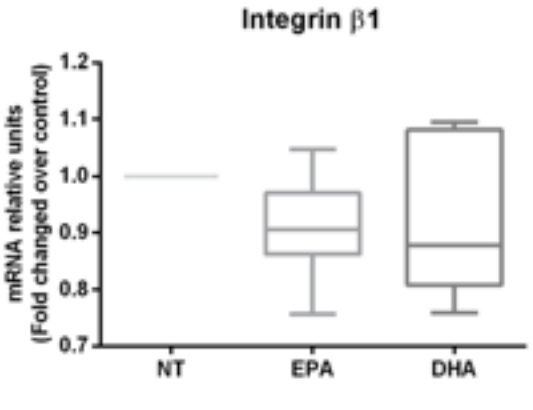

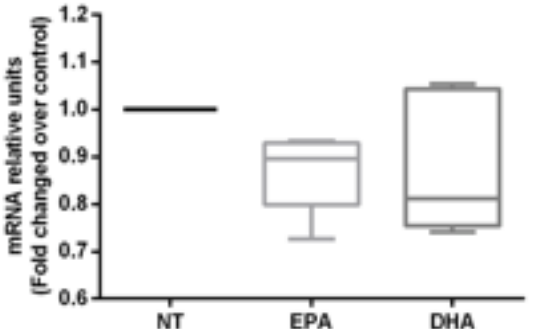

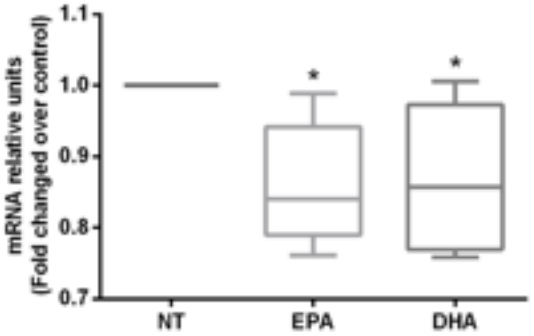

Integrins play an important role in transmitting mechanical signals from the ECM and are characterized as heterodimeric transmembrane receptors.

FAK is phosphorylated in response to integrin engagement, growth factor stimulation, and the action of mitogenic neuropeptides.

Anchor kinase protein 13 (AKAP13) is associated with cytoskeletal filaments.

Effect of EPA and DHA on mRNA expression of sterol regulatory molecules in primary myometrial and leiomyoma cells

ABCG1 and ABCA1 mediate lipid accumulation and are part of the evolutionarily conserved family of ATP-binding cassette cholesterol transporters. ABCG1 and ABCA1 are responsible for the efflux of cholesterol, a precursor of steroid hormones and the fat-soluble vitamins A, D, E, K.

Primary myometrial cells

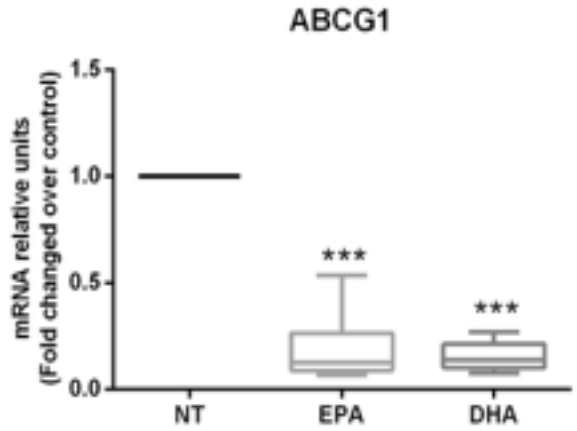

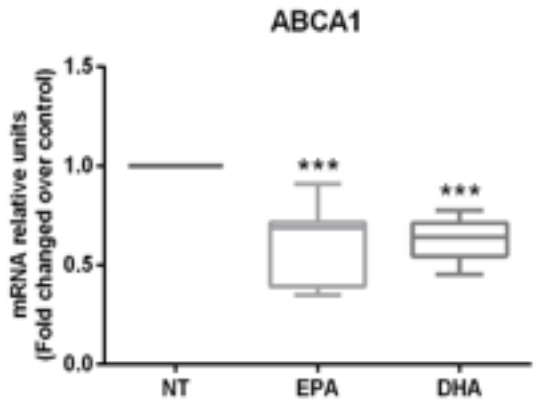

Primary leiomyoma cells

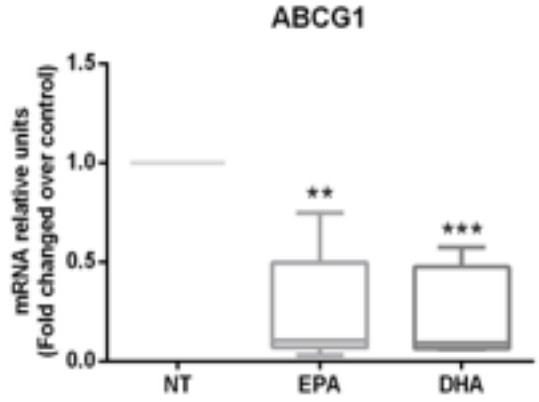

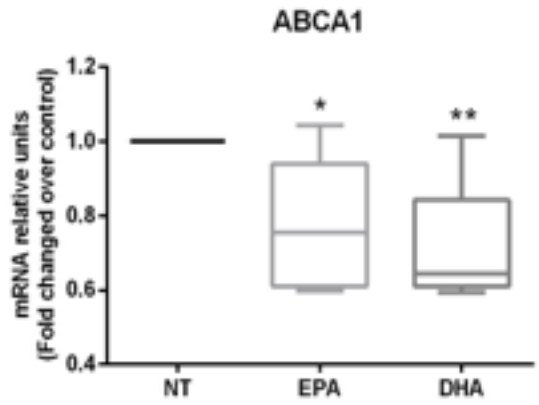

Effect of EPA and DHA on mRNA expression of the mitochondrial enzyme CYP11A1 in primary myometrial and leiomyoma cells

CYP11A1 is a mitochondrial enzyme responsible for catalyzing the conversion of cholesterol to pregnenolone, which is a precursor of estrogens, progestogens, mineralocorticoids, glucocorticoids, and androgens.

Primary myometrial cells

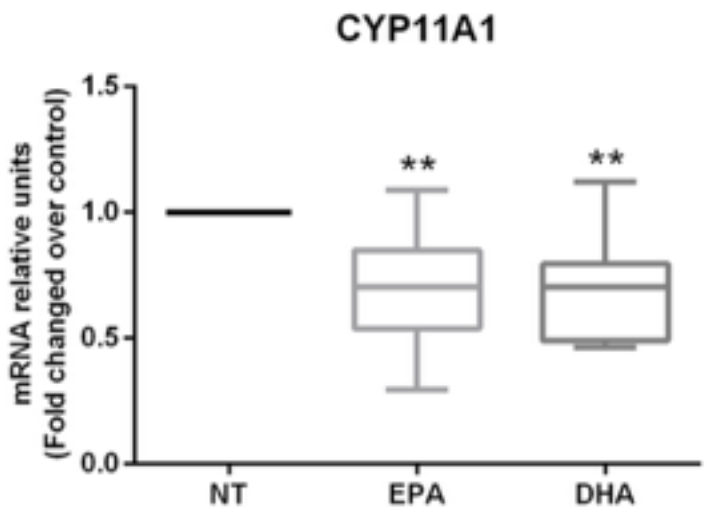

Primary leiomyoma cells

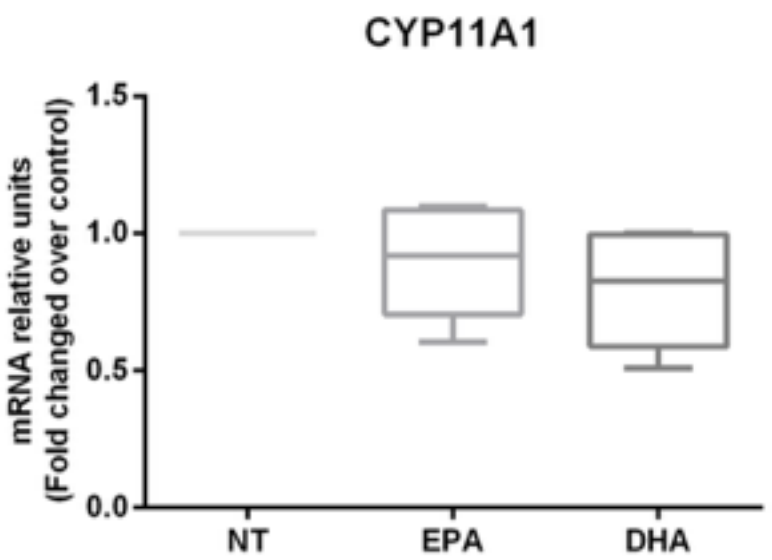

Islam MS, Castellucci C, Fiorini R, Greco S, Gagliardi R, Zannotti A, Giannubilo SR, Ciavattini A, Frega NG, Pacetti D, Ciarmela P. Omega-3 fatty acids modulate the lipid profile, membrane architecture, and gene expression of leiomyoma cells. J Cell Physiol. 2018 Mar 25

Conclusions

The ECM synthesis and dysregulation are important events in leiomyoma growth.

Uterine fibroids may have inflammatory/reparative pathogenesis.

Involvement of cell membrane and lipid content.

Collaborations

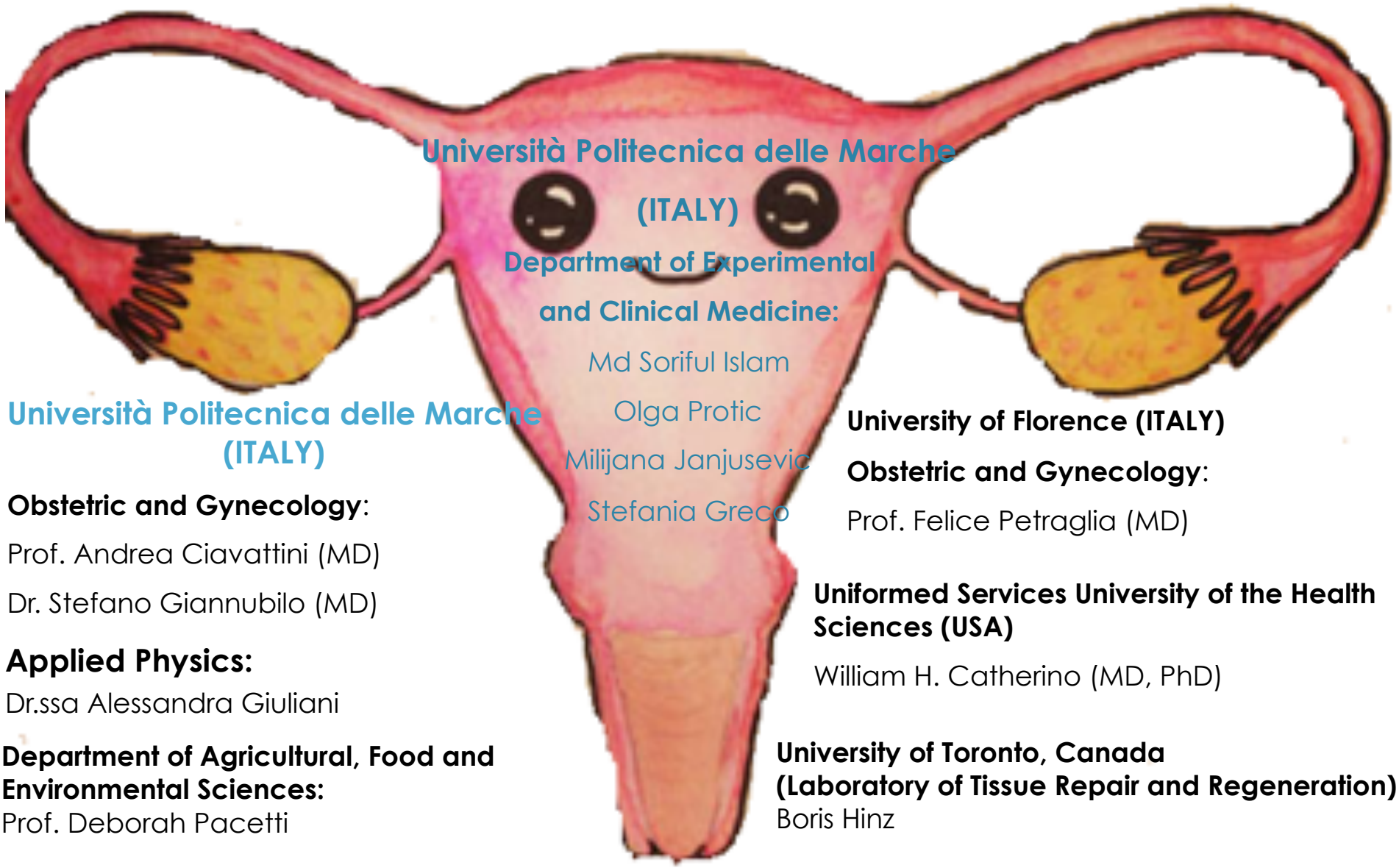

Università Politecnica delle Marche (ITALY)

Department of Experimental and Clinical Medicine:

Md Soriful Islam

Olga Protic

Milijana Janjusevic

Stefania Greco

Università Politecnica delle Marche (ITALY)

Obstetric and Gynecology:

Prof. Andrea Ciavattini (MD)

Dr. Stefano Giannubilo (MD)

Applied Physics:

Dr.ssa Alessandra Giuliani

Department of Agricultural, Food and Environmental Sciences:

Prof. Deborah Pacetti

University of Florence (ITALY)

Obstetric and Gynecology:

Prof. Felice Petraglia (MD)

Uniformed Services University of the Health Sciences (USA)

William H. Catherino (MD, PhD)

University of Toronto, Canada (Laboratory of Tissue Repair and Regeneration)

Boris Hinz

Department of Life and Environmental Sciences:

Dr.ssa Rosamaria Fiorini